The high-redshift Universe and the role of galaxies and AGN to cosmic reionization

Lecture 2

- Selection techniques of high-redshift AGN
- The census of early SMBHs: what we know and what we miss
- Nuclear obscuration at high redshift

Roberto Gilli
INAF – Osservatorio Astronomico di Bologna

Optical and near-IR selection: the “dropout” technique

Reionization and IGM transmission

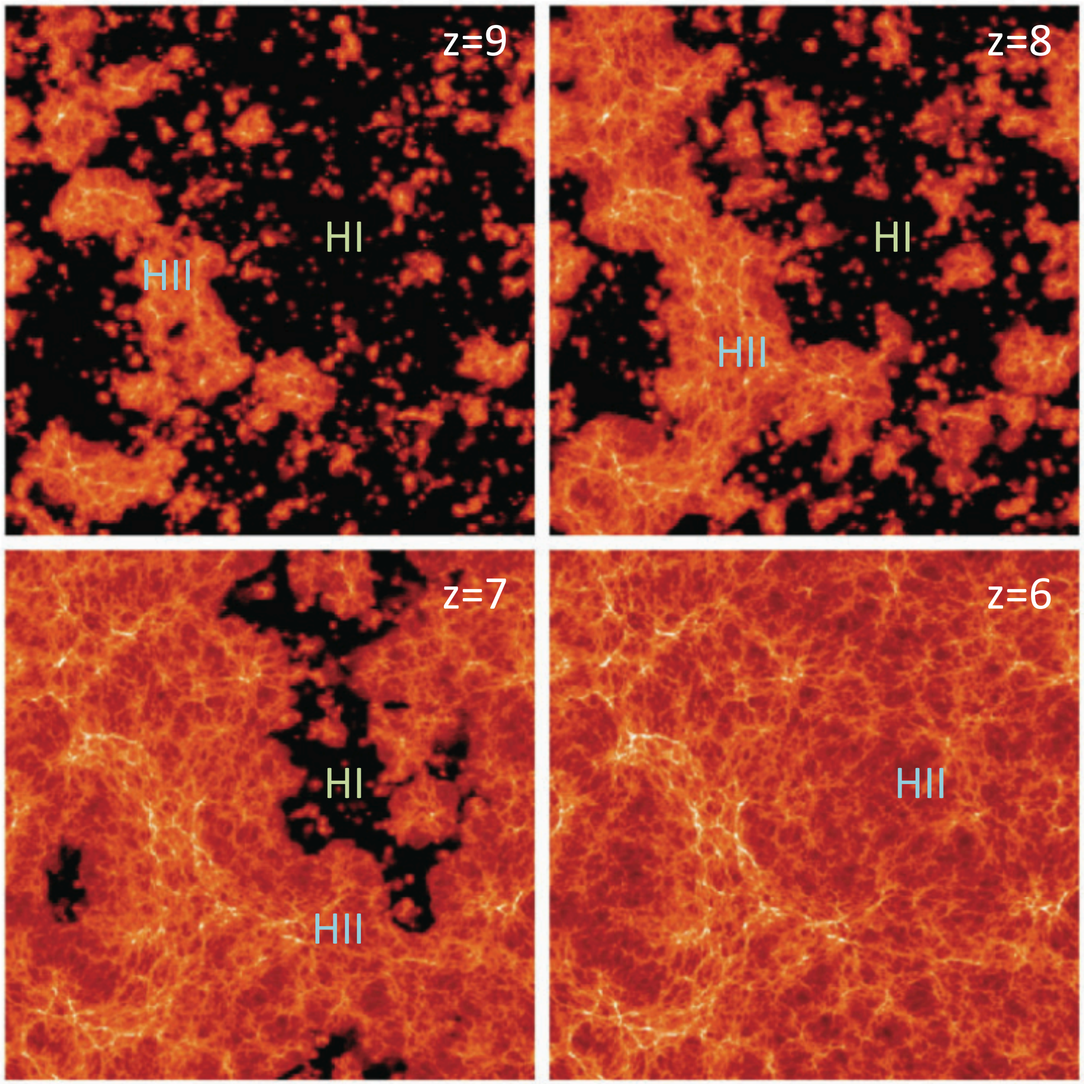

Moving back in time the fraction of neutral hydrogen increases and the IGM becomes progressively more opaque to photons with λ_{rest}<1216 Å

average HI fraction is < 10^{-4} at z~6

Trac & Cen 2007

The Lyman alpha forest

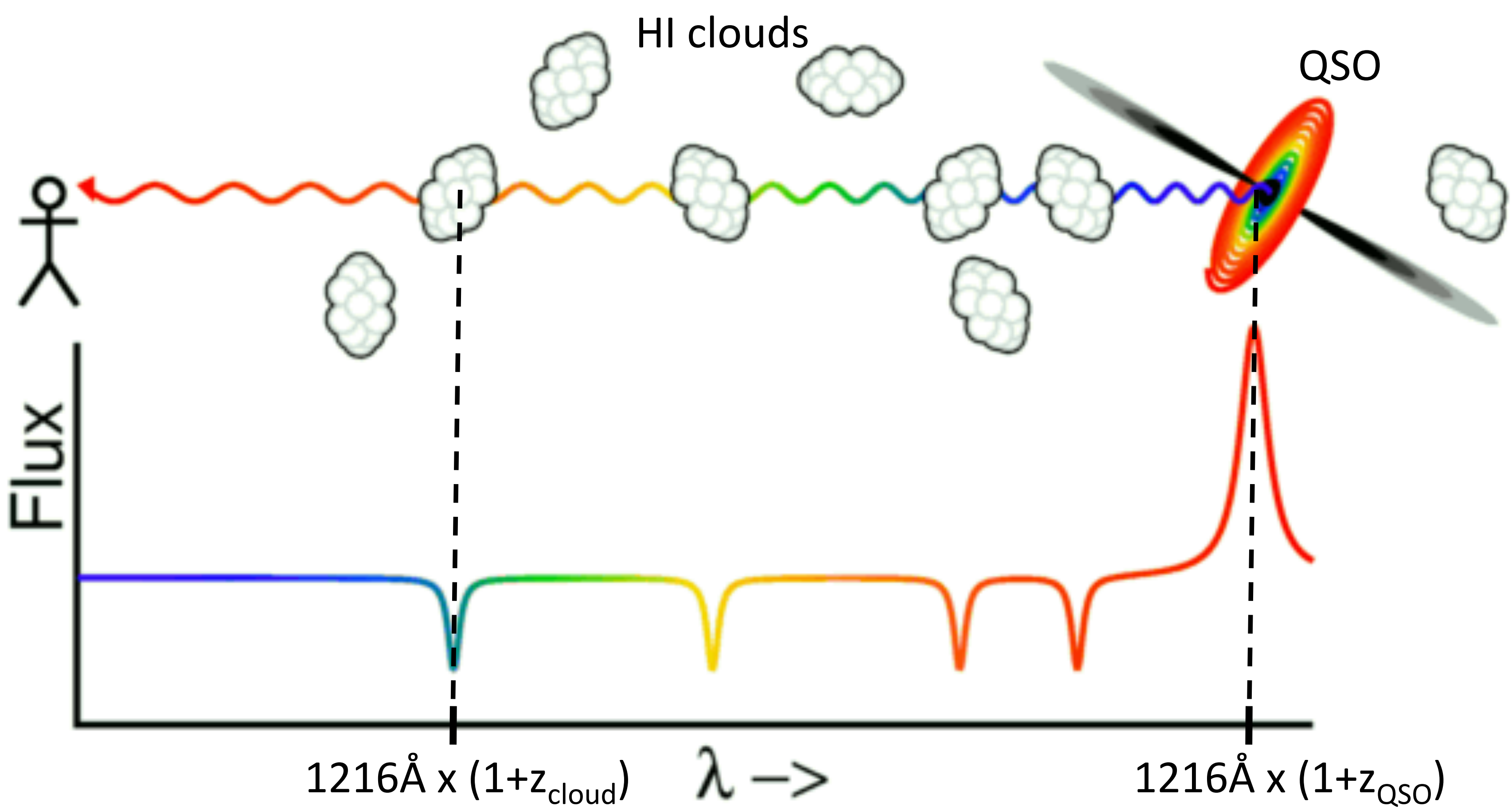

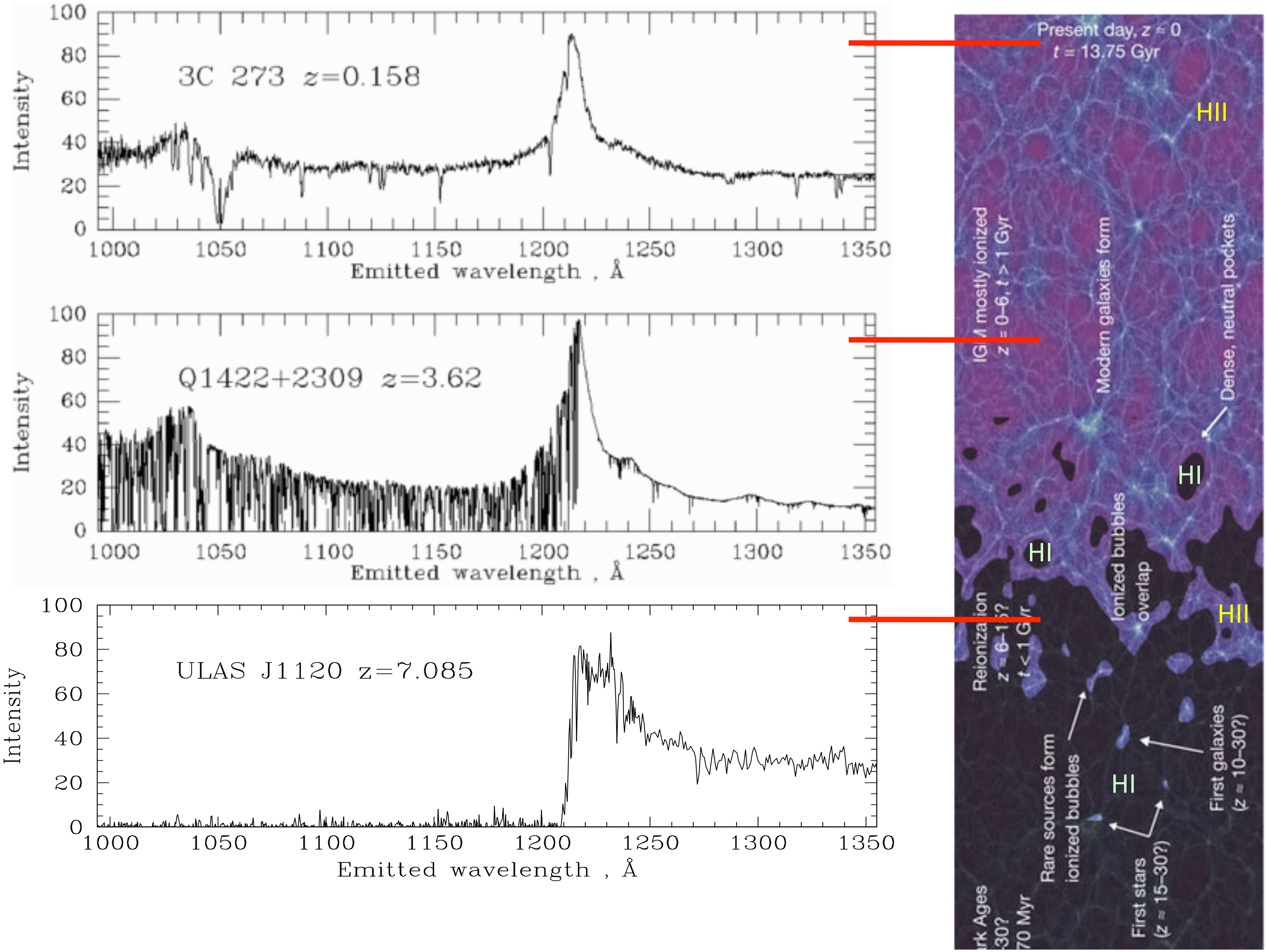

3C 273 z=0.158
Q1422+2309 z=3.62
ULAS J1120 z=7.085
Intensity
Emitted wavelength , Å
Present day, z ≈ 0
t = 13.75 Gyr
HII
HI
IGM mostly ionized
z = 0–6, t > 1 Gyr
Modern galaxies form
Dense, neutral pockets
Ionized bubbles overlap
Reionization
Rare sources form ionized bubbles
First galaxies (z ≈ 10–30?)
First stars (z ≈ 15–30?)

QSOs at z~6 appear as "i-band dropouts"

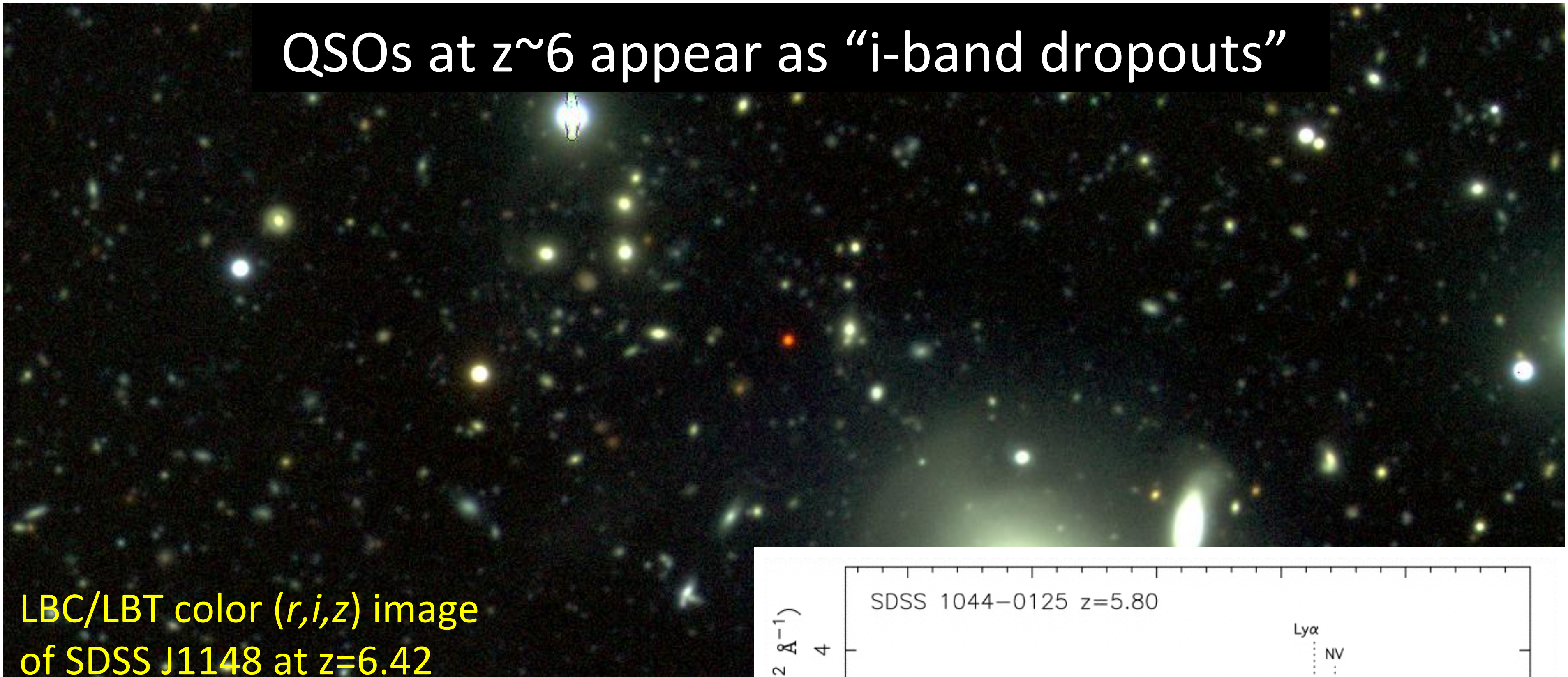

LBC/LBT color (*r,i,z*) image of SDSS J1148 at z=6.42

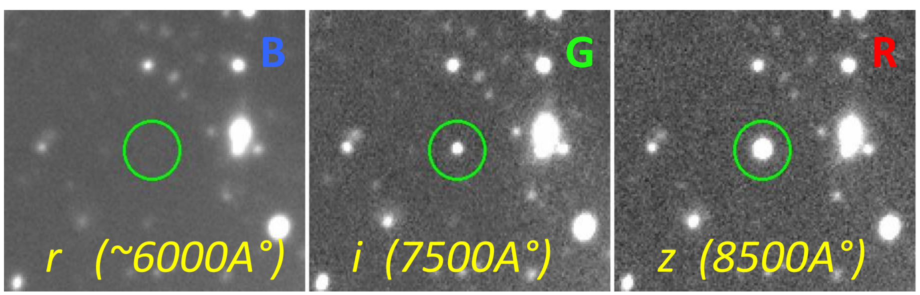

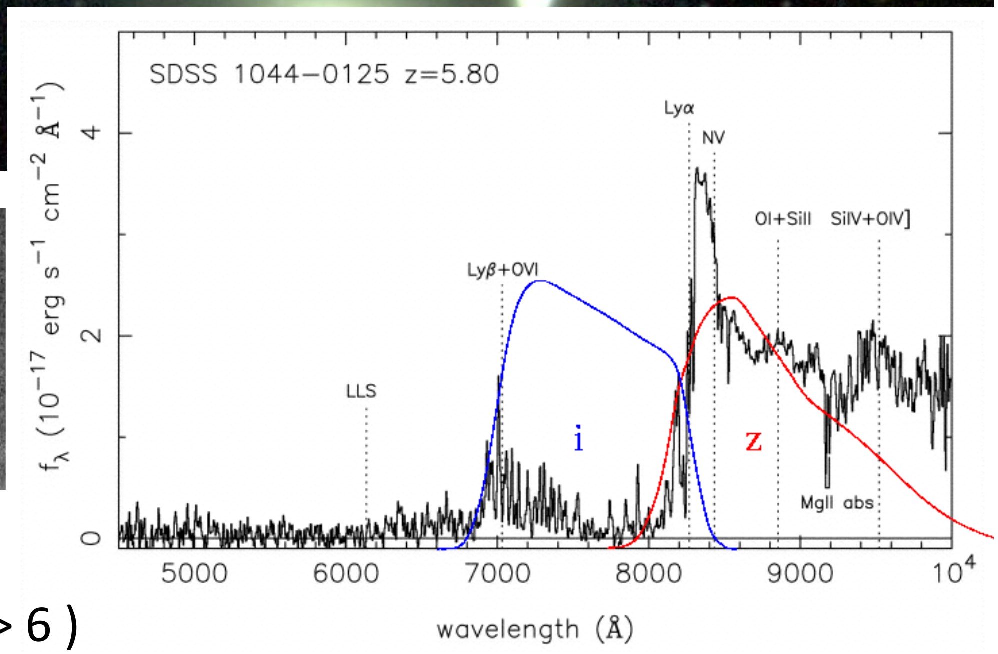

Color selection: i-z >~ 2.0 (~ $f_{8500}/f_{7500} > 6$)

no detection blueward of i-band

Fan et al. 2001

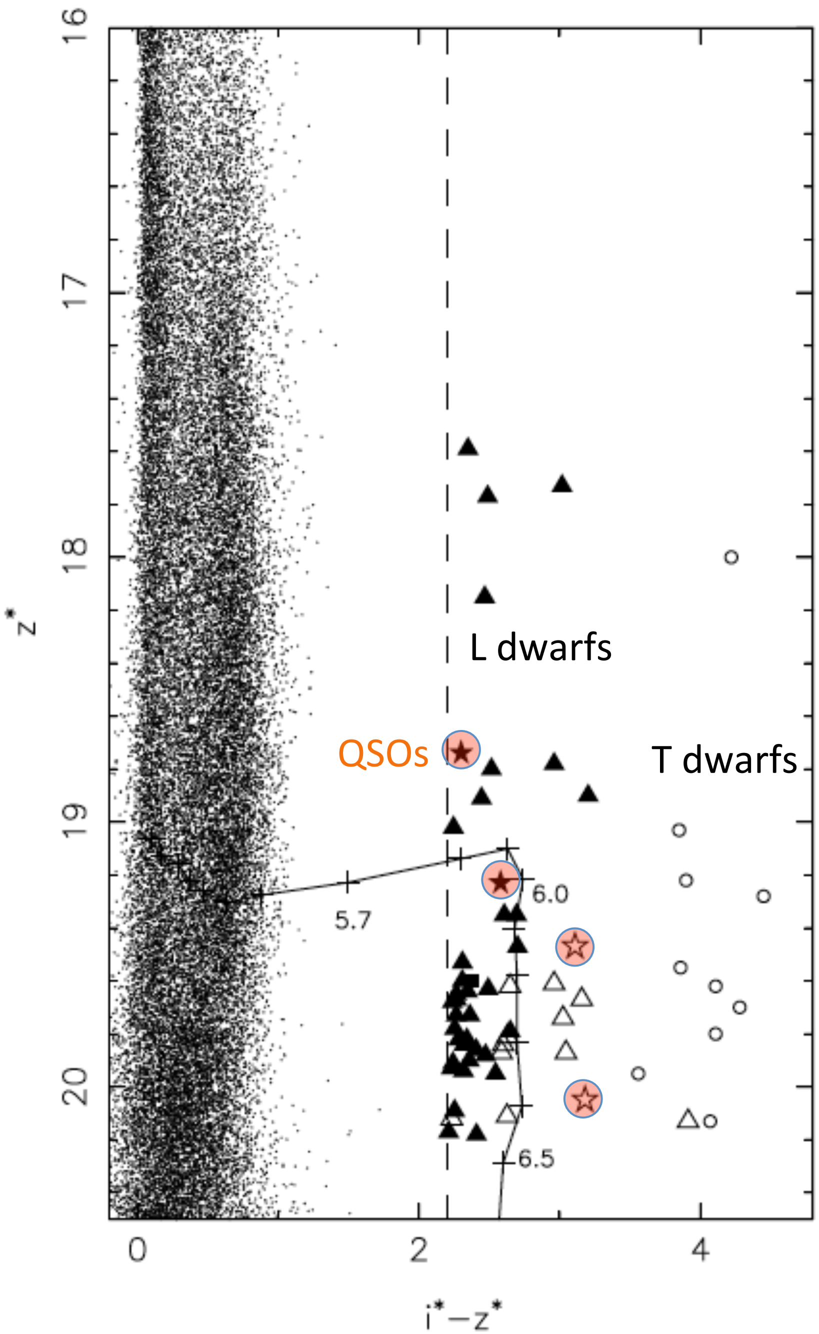

late type stars are the most abundant pointlike sources in the sky

Contaminants: cool (T<~3500K) dwarfs (M, L, T)

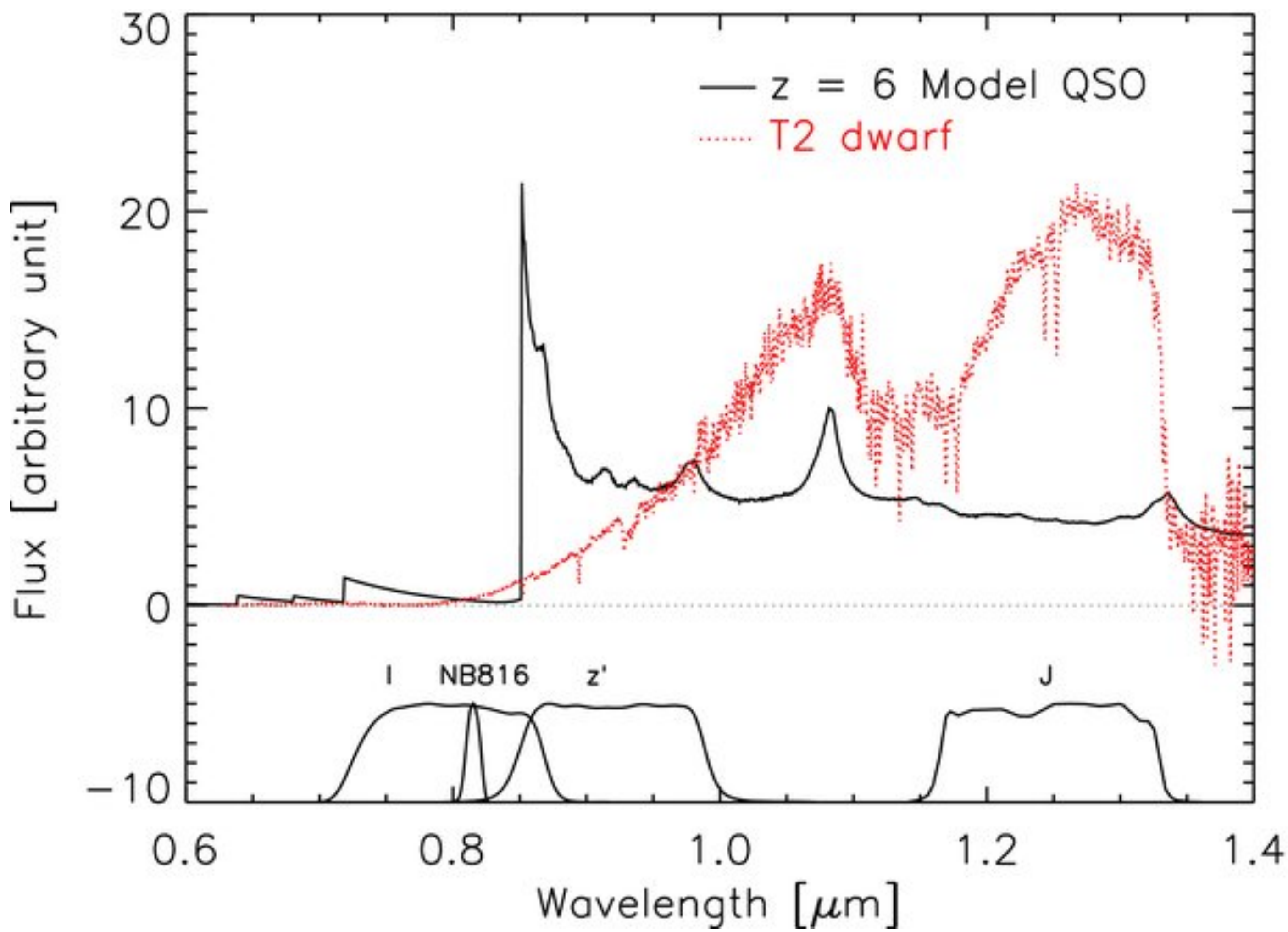

Late type stars have similar i-z colors to z~6 QSOs but much redder z-J colors

Removing stellar contaminants with near-IR (e.g. J-band) imaging

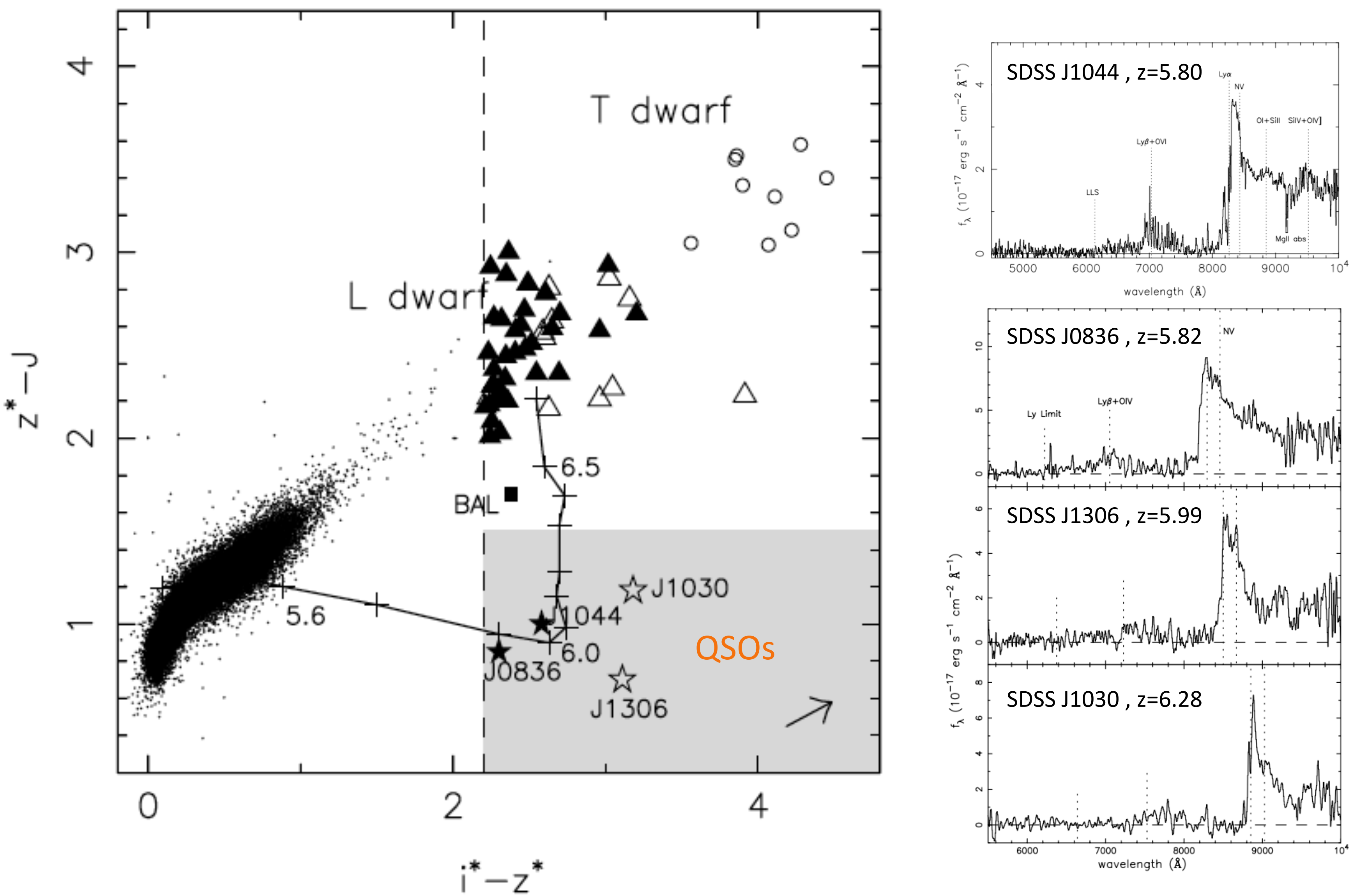

Fan et al. 2001

The SDSS breakthrough

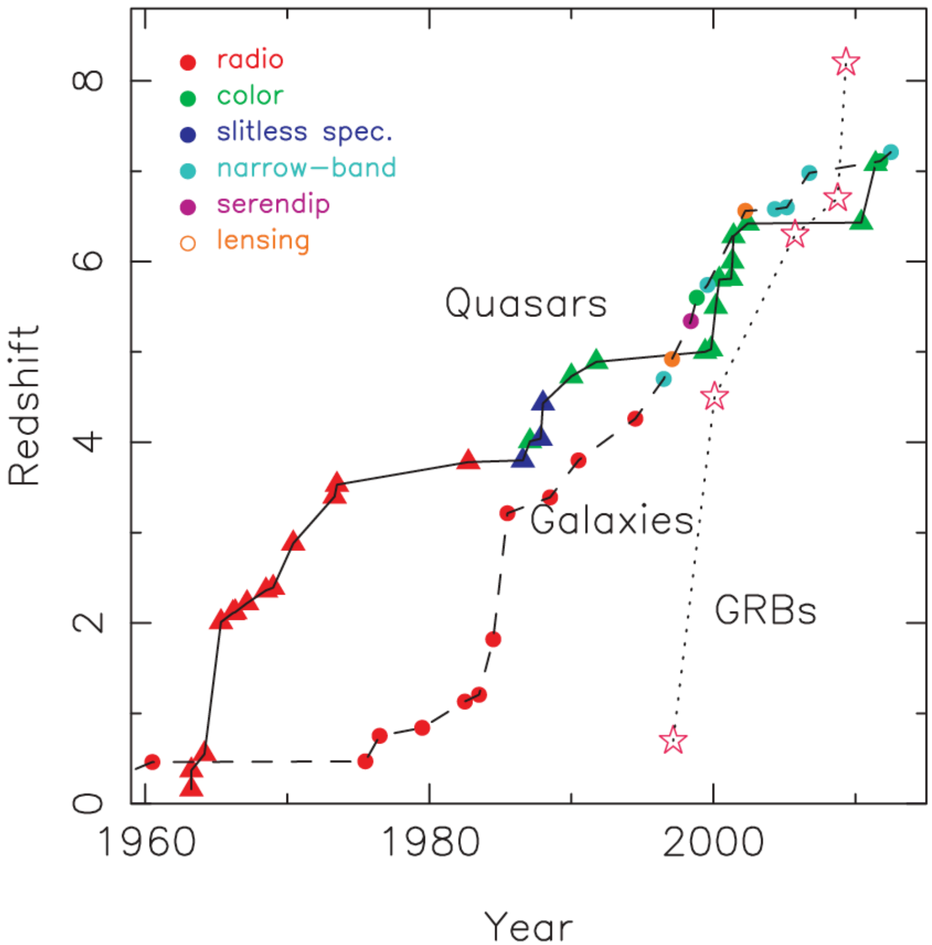

Fan 2012

SDSS DR12 imaging coverage

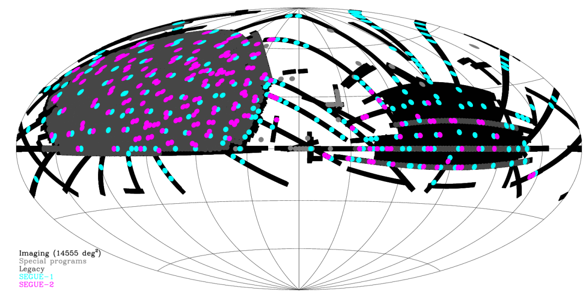

>14,000 deg^2 *ugriz* imaging in SDSS DR12 selection of bright (z_{AB}<20) QSOs up to z~6.5 (i-band dropouts) possible over ~1/3 of the sky

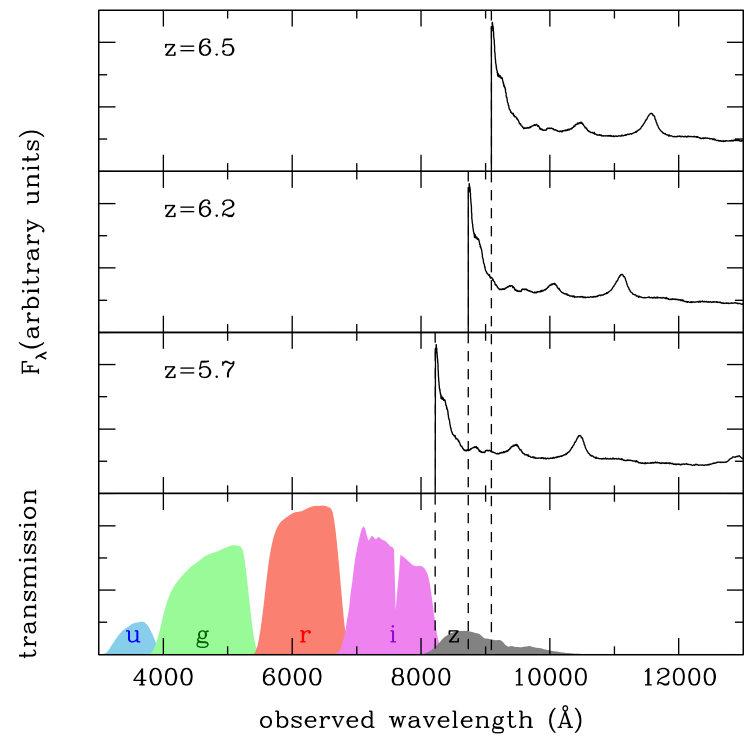

Beyond redshift 6.5:near-IR imaging and z-band dropouts

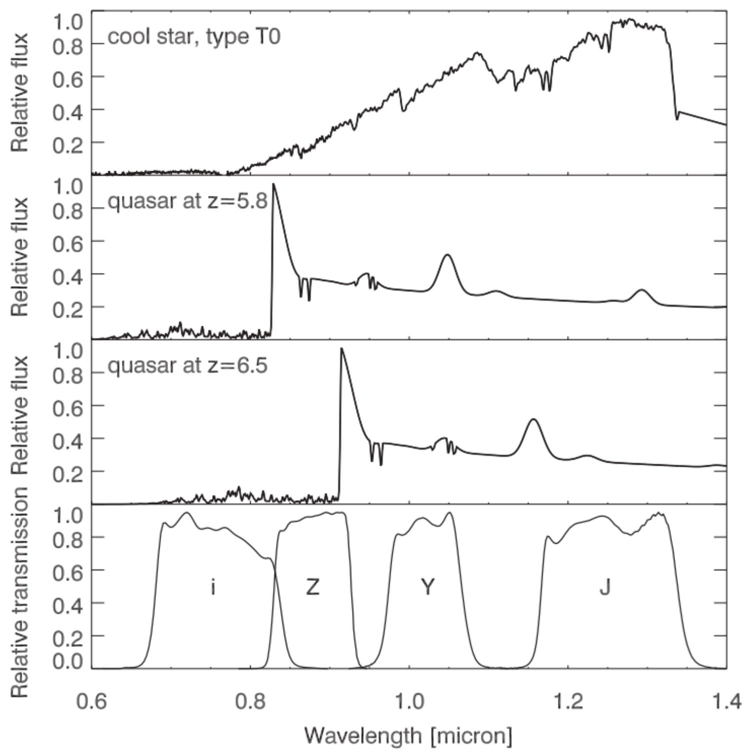

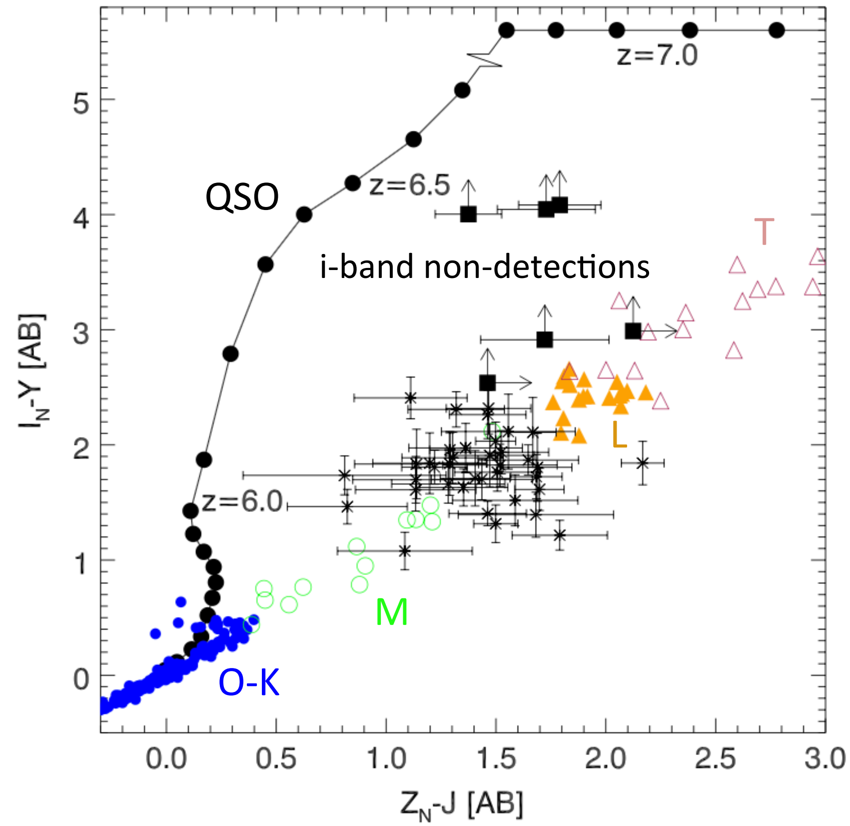

VIKING survey: zYJHKs 1500 deg^2
selects QSO candidates with $6.5<z<7.4$ and $Y_{AB}< 21.3$

Venemans et al. 2013, 2015

3 QSOs at z>6.5 discovered in VIKING

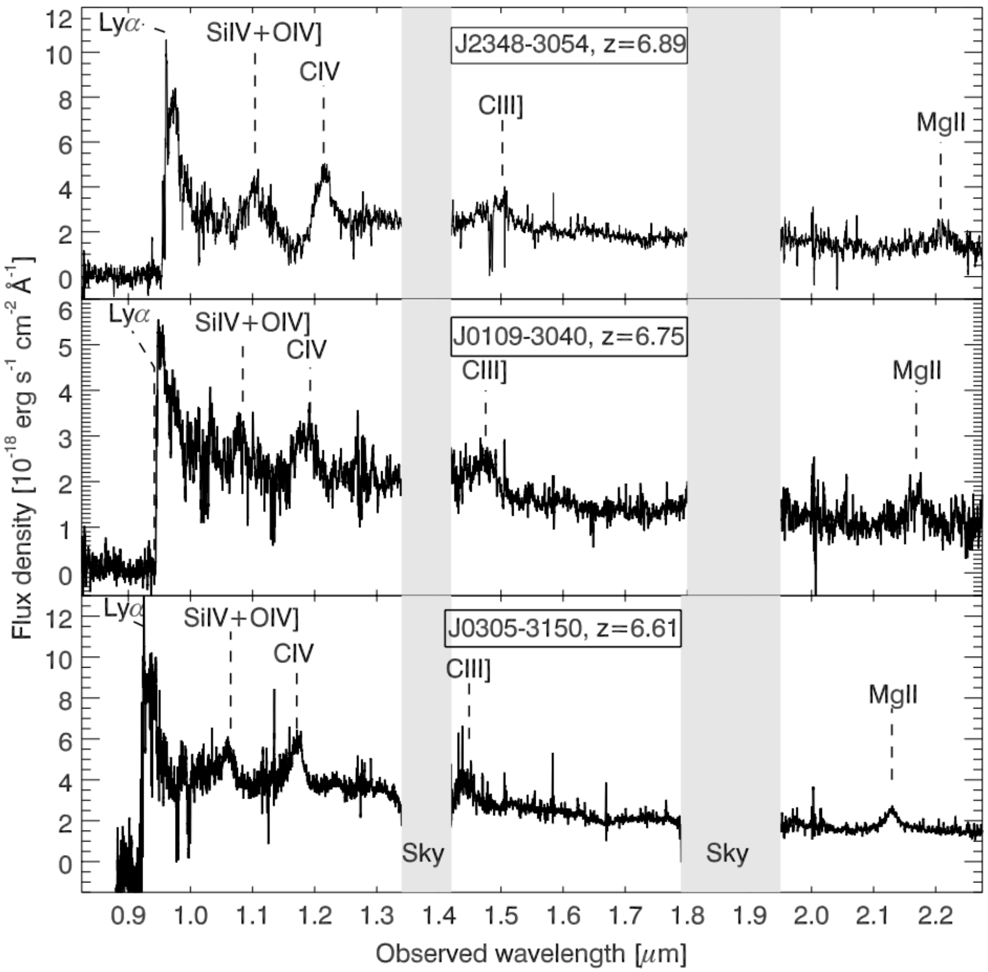

total of 7 QSOs at z>6.5 known to date

including

1 (ULASJ1120 at z=7.085) from UKIDSS LAS:
4000 deg^2, YJHK,
z-band dropouts down to Y_{AB}~20.2

3 (Venemans et al. 2015) from Pan-STARRS:
20000 deg^2, grizY,
z-band dropouts down to Y_{AB}~20.5

Venemans et al. 2013

Demography of high-z QSOs

About **80 QSOs known at z>5.7** from wide areaoptical (SDSS, CFHQS, Pan-STARRS1) and near-IR (UKIDSS, VISTA) surveys

SDSS main and PS1 trace the brightest QSOs: M_{1450} ~ −27, L_{bol} ~ 3 x 10^{47} L_{sun}

SDSS-Stripe82 and CFHQS ~2 mag deeper

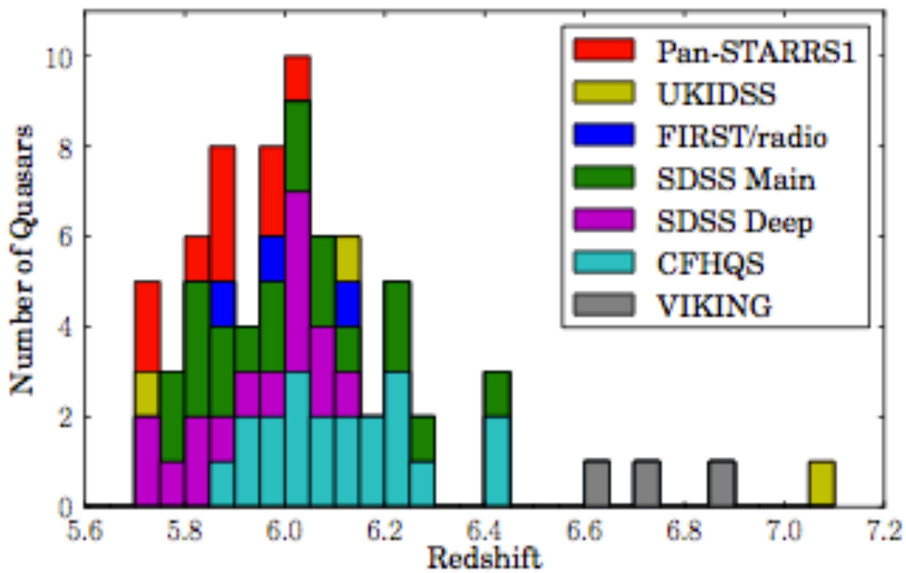

Banados et al. 2014

Fan 2012

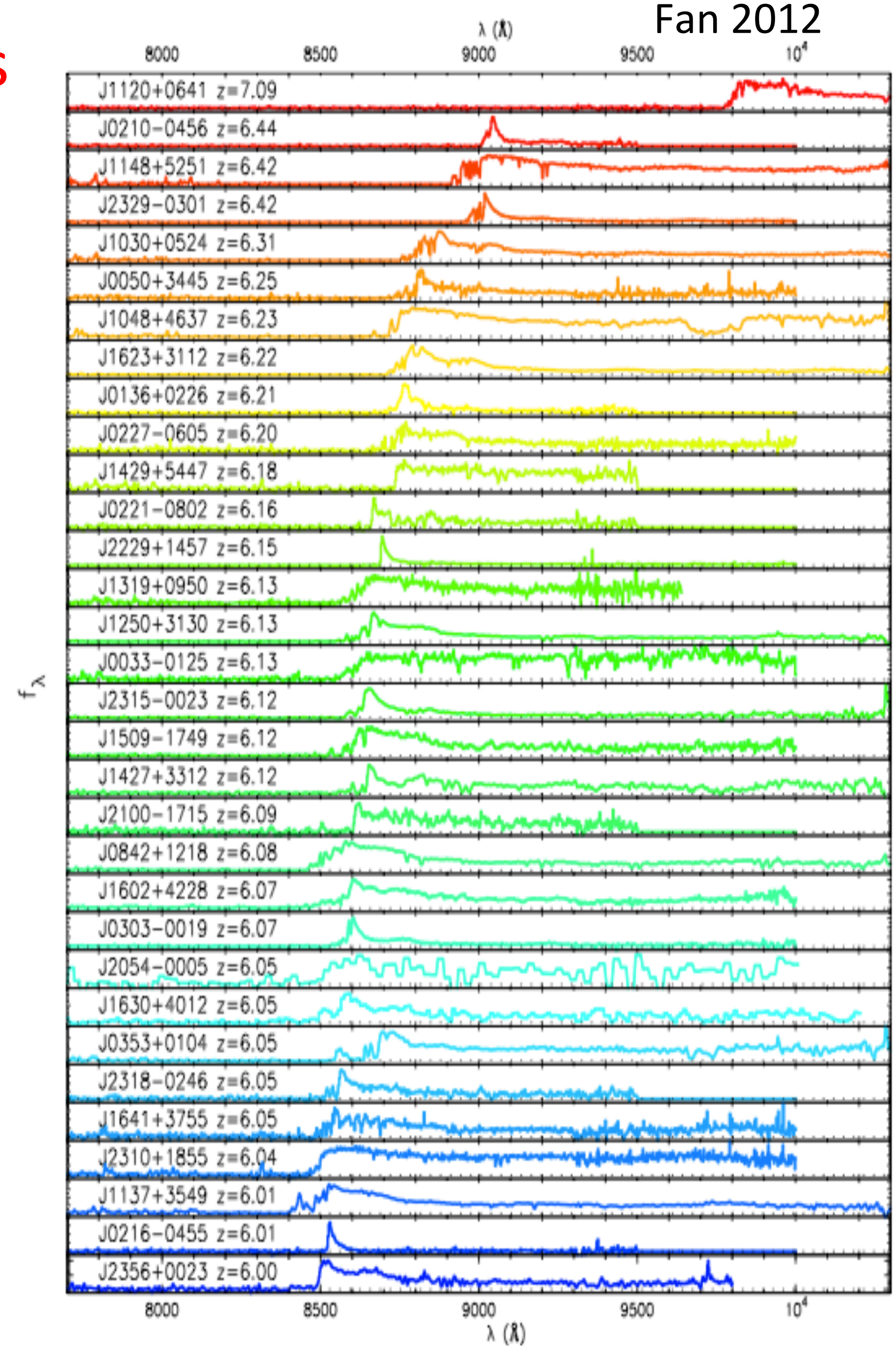

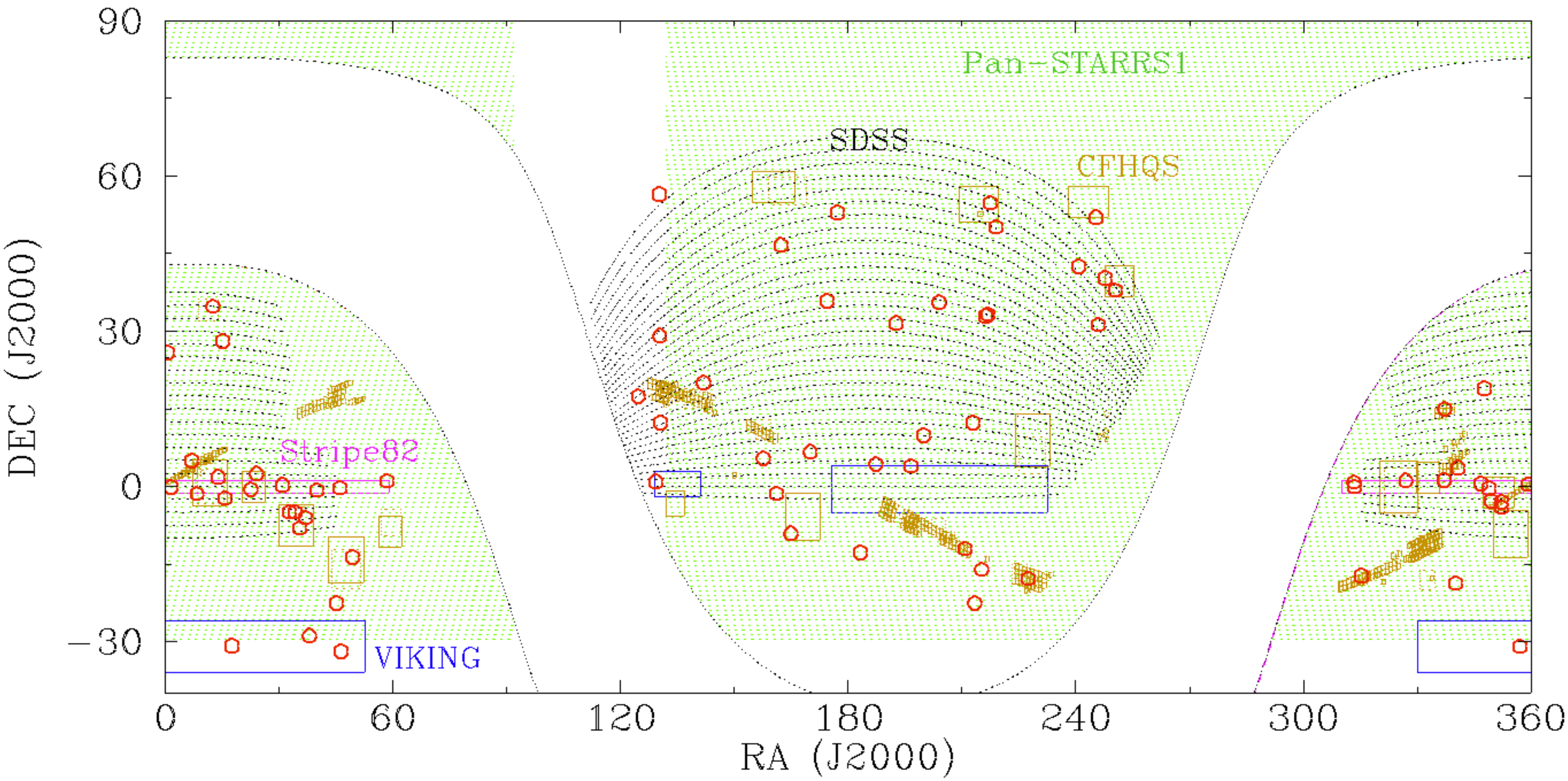

~ 1 every 500 deg^2 at z_{AB}<20 (➔ only ~80 in the whole Universe)
~ 1 every 40 deg^2 at z_{AB}<22

Evolution of luminous QSOs

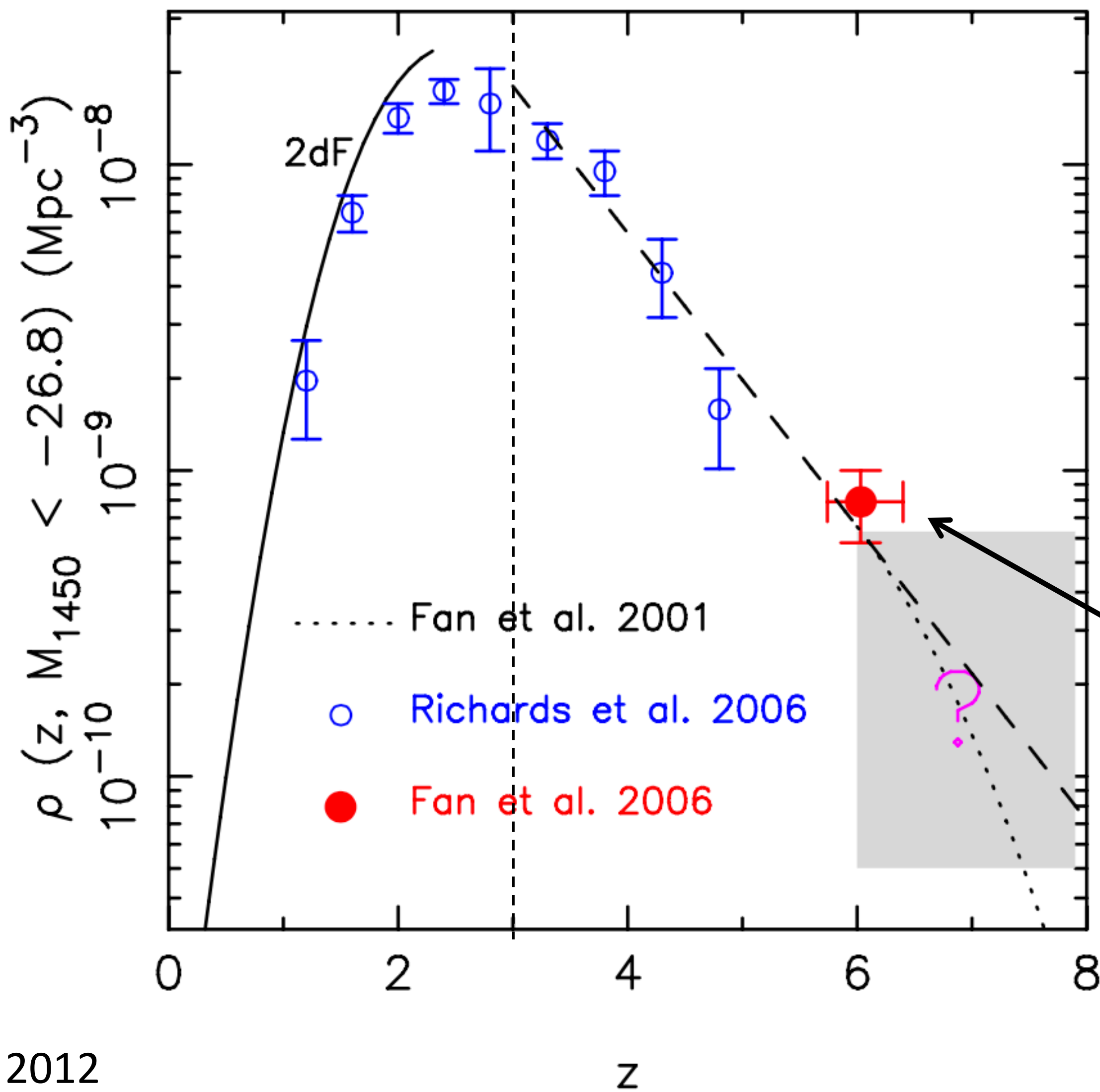

$M_{1450} < -26.8$

i.e.

$L_{bol} > 3 \times 10^{47}$ erg/s

$L_{bol} > 7.5 \times 10^{13}\ L_{sun}$

$M_{BH} > 2 \times 10^{9}\ \lambda_{Edd}^{-1}\ M_{sun}$

$\lambda_{Edd} = L_{bol}/L_{Edd}$

~ 1 per Gpc^3 (rare)

difficult to simulate

Fan 2012

Luminosity Function of z~6 QSOs

less than 3 AGN with M_{1450} > -23 known at z~6
(M_{BH} > 4 x 10^7 λ_{Edd}^{-1} M_{sun})

none with M_{1450} > -22
(M_{BH} > 1.5 x 10^7 λ_{Edd}^{-1} M_{sun})

faint end slope still extremely uncertain

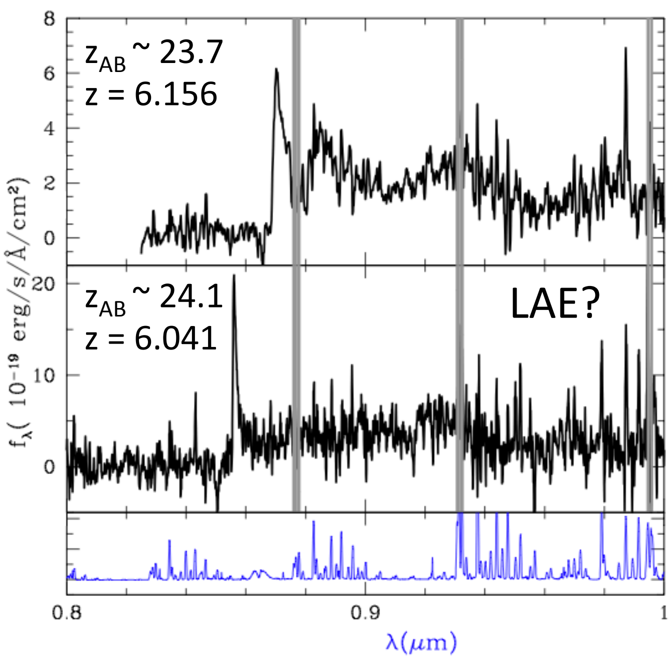

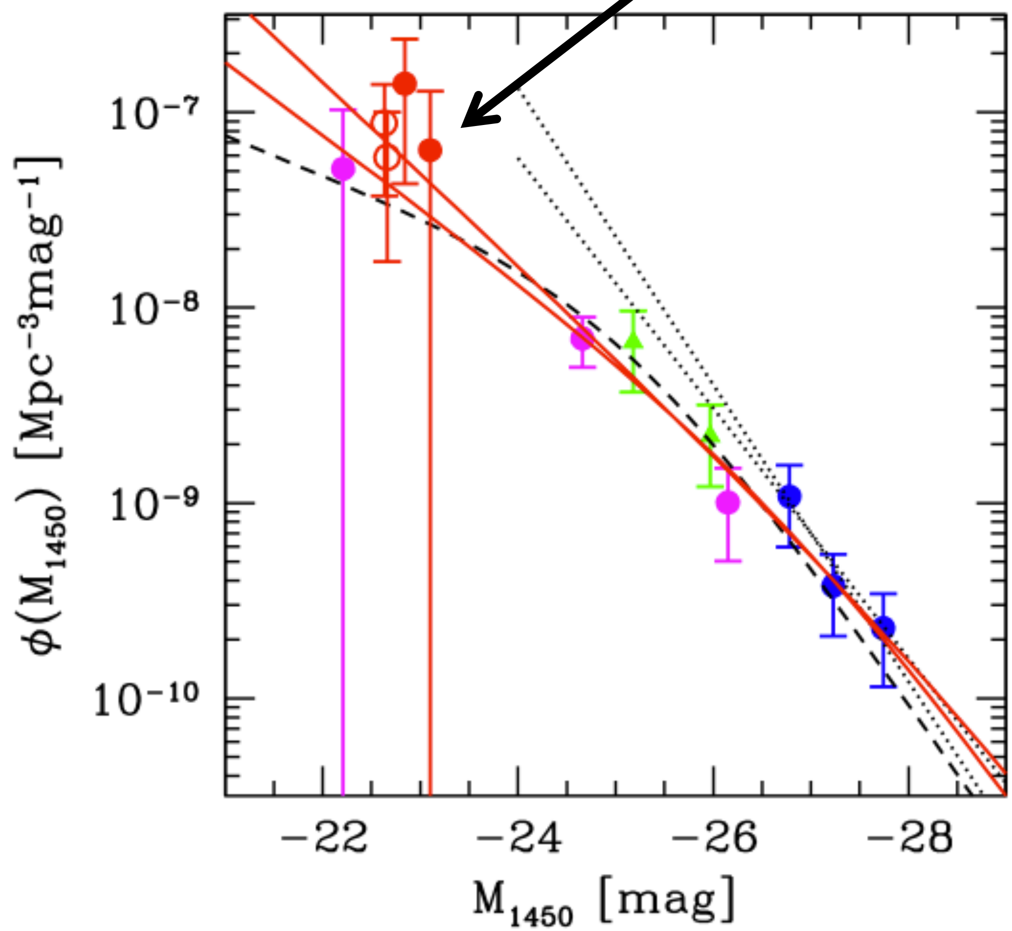

Kashikawa et al. 2014

Are we just seeing the tip of the iceberg?

How many low-lum (small BHs) and distant AGN do we miss?

How do we detect them and distinguish among the various seeding and fueling models?

What if the nucleus is hidden?
How many obscured and distant AGN do we miss?

The largest AGN population: hidden accreting SMBHs

AGN types: (type 1) unobscured vs (type 2) obscured

Mignoli et al. 2013

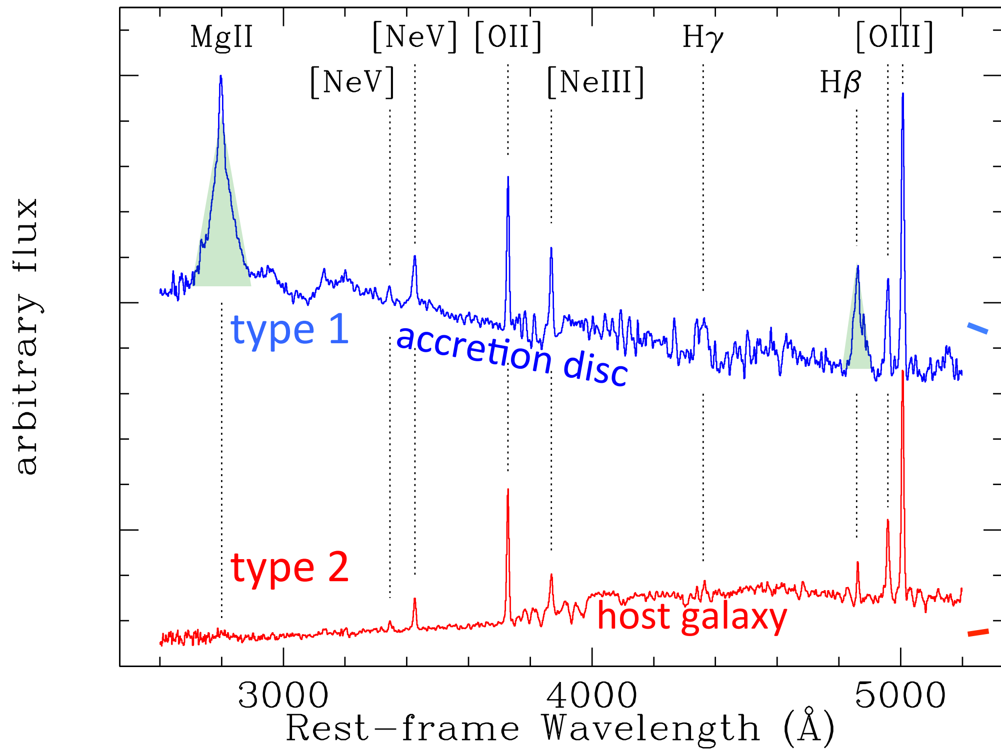

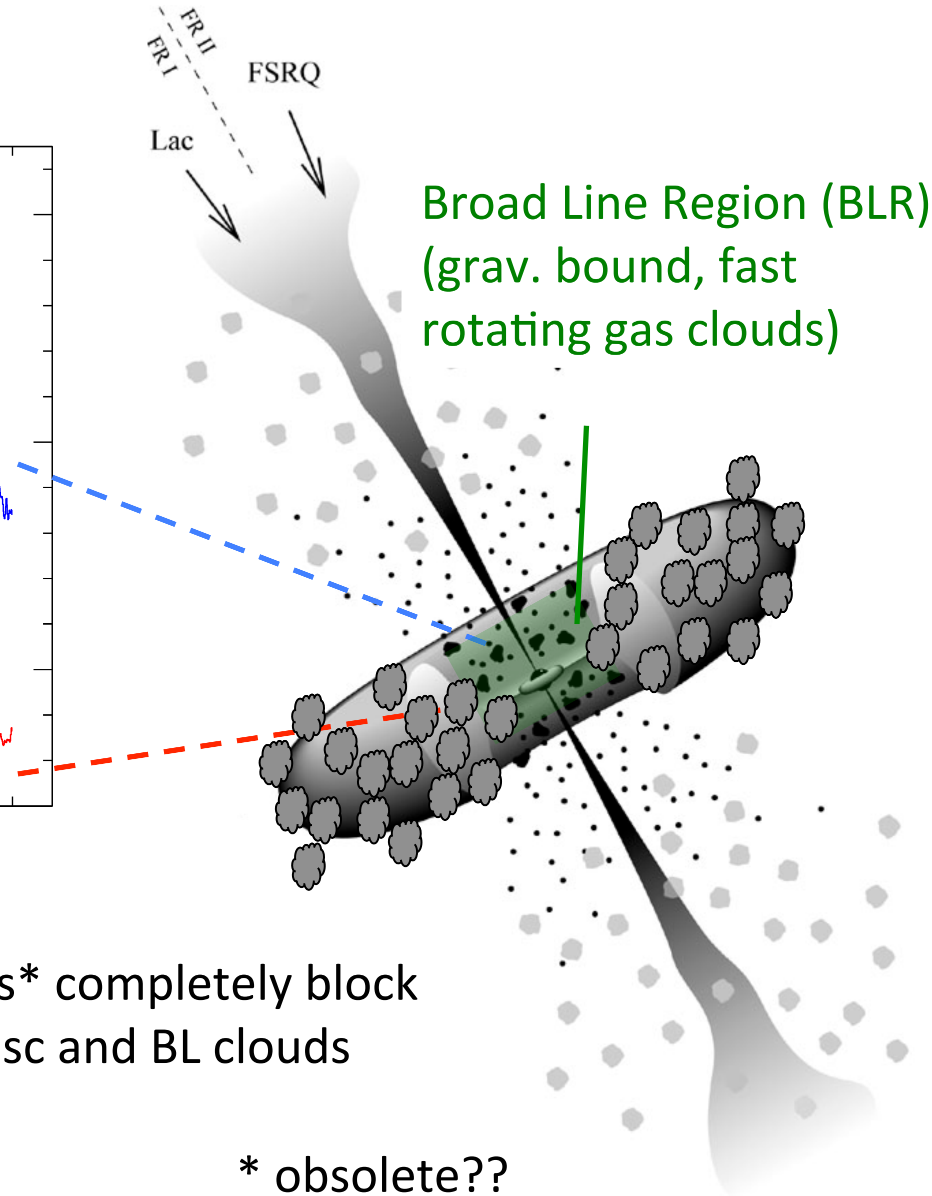

dust and gas in the pc-scale obscuring torus* completely block the UV/optical radiation of the accretion disc and BL clouds

* obsolete??

ACS i-band images of AGN at z=1.6 ➔ 3000Å rest-frame

type 1 (direct view of the nucleus: pointlike)

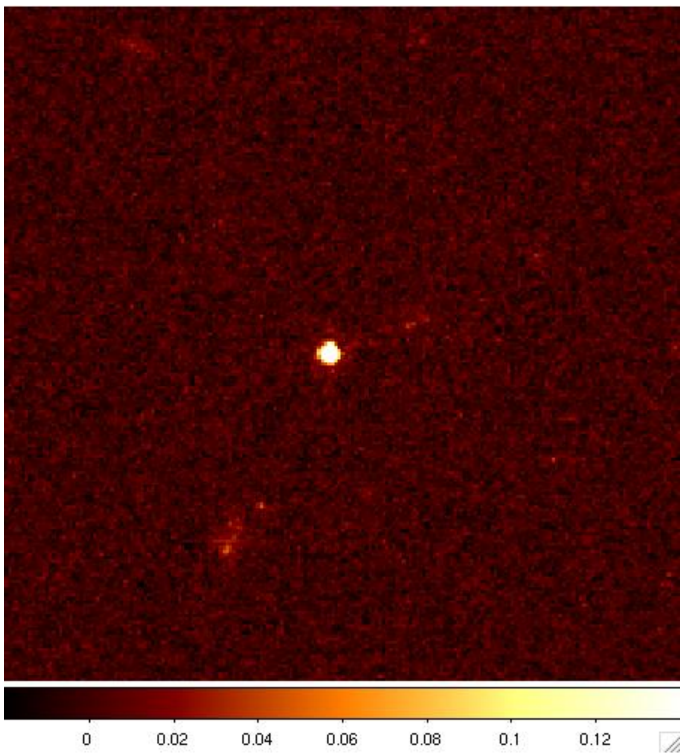

type 2 (only host visible: extended)

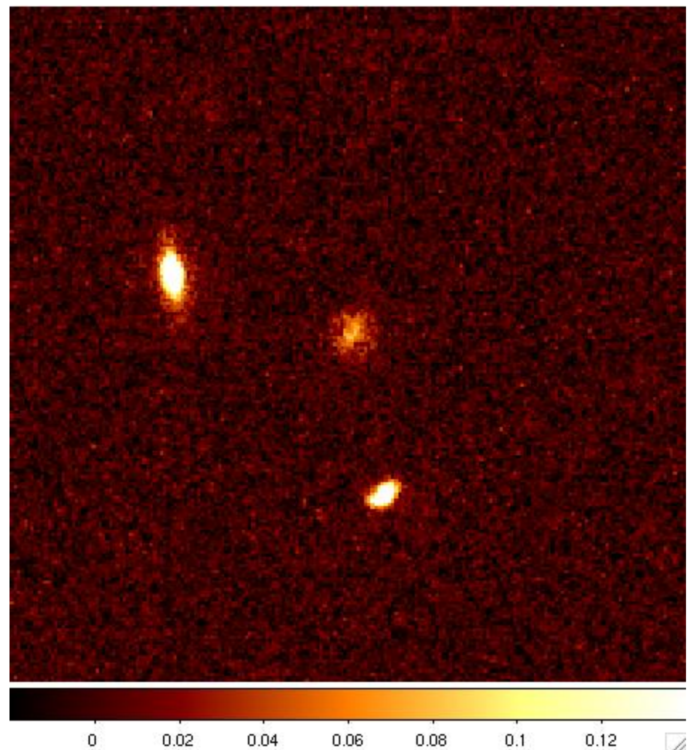

optical imaging not efficient to select obscured AGN

➔ use X-rays: largely free from absorption (especially at high-z) and galaxy dilution

Courtesy M. Mignoli

Examples of X-ray spectra of nearby AGN

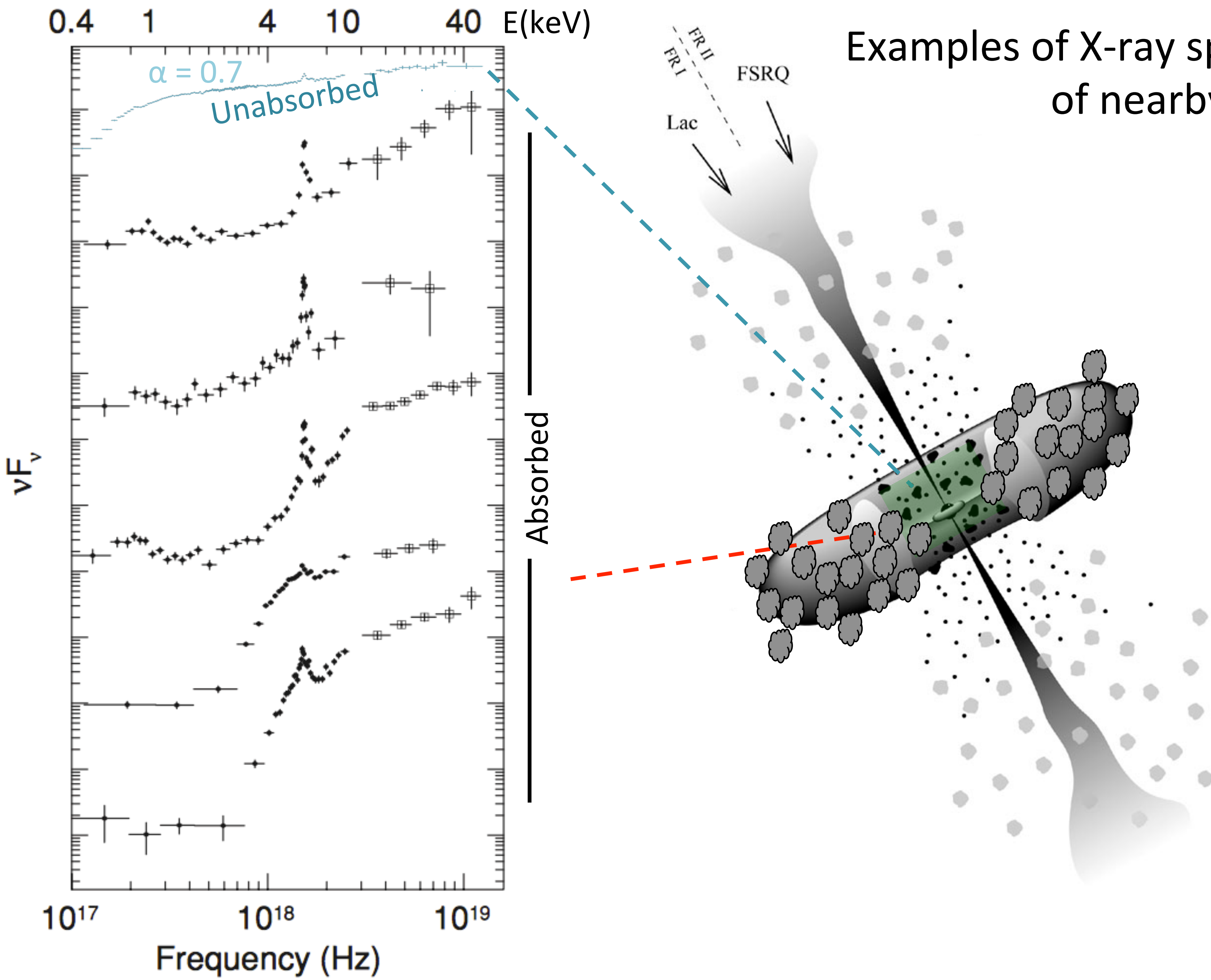

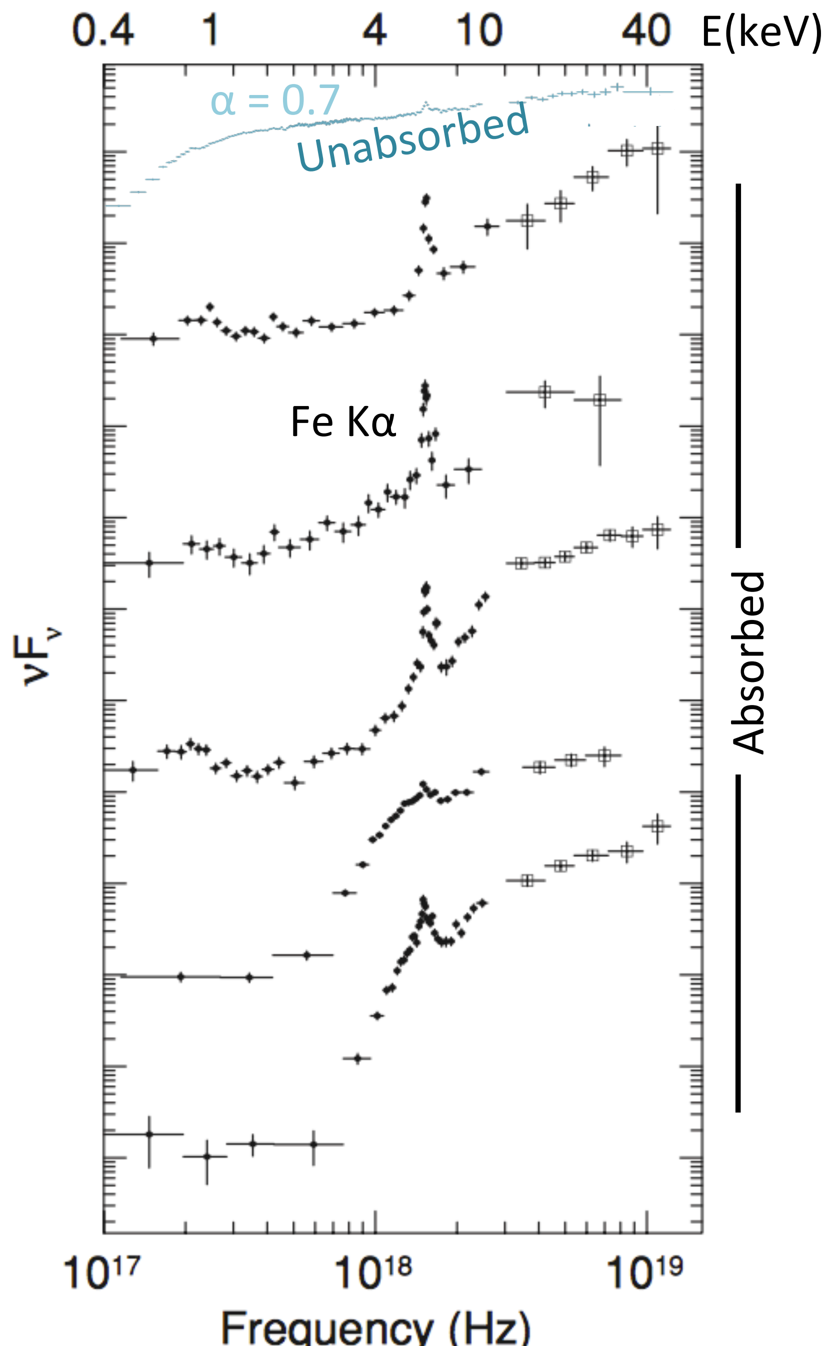

Examples of X-ray spectra of nearby AGN

Unabsorbed (intrinsic)

$I_{Int}(E) \approx E^{-\alpha}$ α = 0.7 - 1.0

($N_{Int}(E) \approx E^{-\Gamma}$ Γ = 1.7 - 2.0)

Absorbed

$I_{Abs}(E) \approx I_{Int}(E)\, e^{-\tau}$

$\tau = N_H \sigma_E$

Fe Kα (@ 6.4 keV for neutral iron) fluorescence within "torus"

Adapted from Comastri et al. 2010

Cross sections

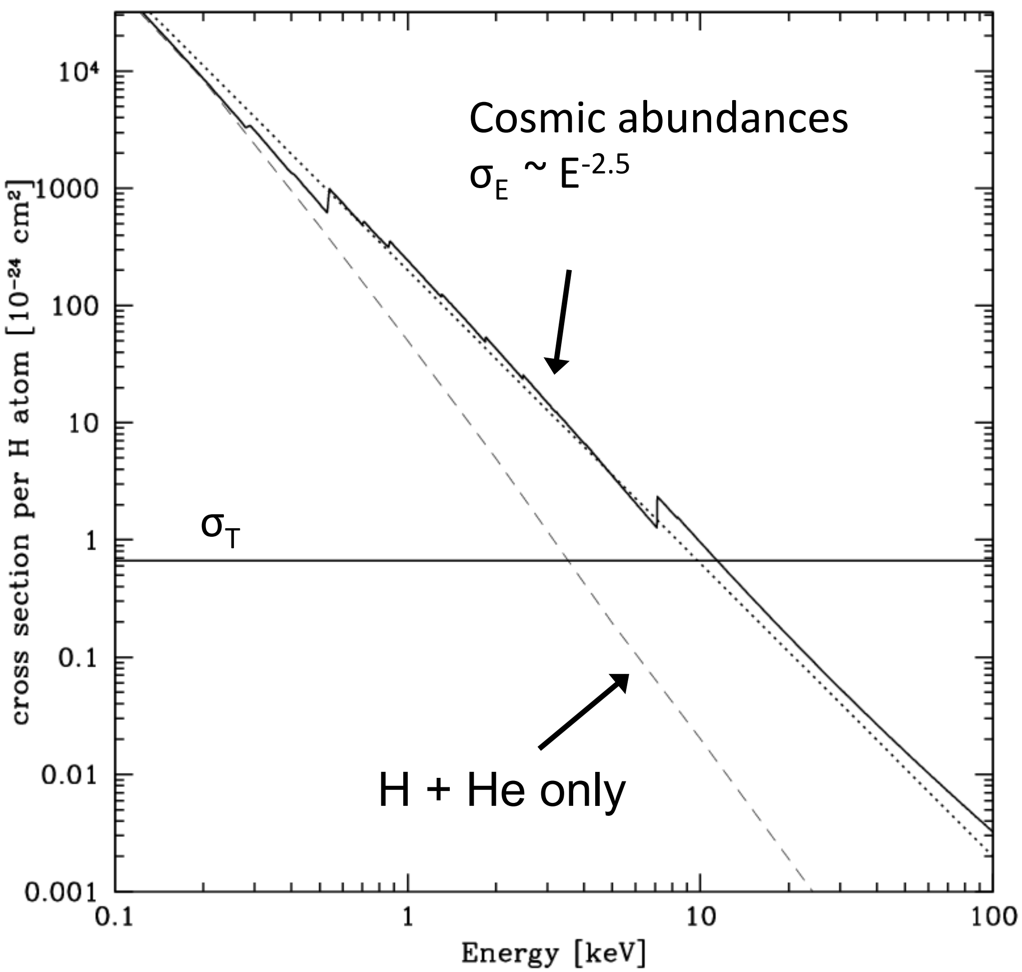

example: for $N_H=10^{23}$ cm^{-2}, absorption at 2 keV by gas with cosmic abundance of metals is 90 times more efficient than by metal-free gas

σ_E = cross section for photoelectric absorption
σ_T = cross section for Thomson scattering

N_H = hydrogen equivalent column density
units : cm^{-2}

$I_{obs}(E)/I_{int}(E) \approx e^{-\tau}$
$\tau = N_H \sigma_E$
$\sigma_E \approx E^{-2.5}$ ➔
Nuclear emission is transparent at high energies

Absorption of X-ray photons is produced by metals

$\sigma_T > \sigma_E$ at E> 10 keV

Photoelectric absorption + scattering

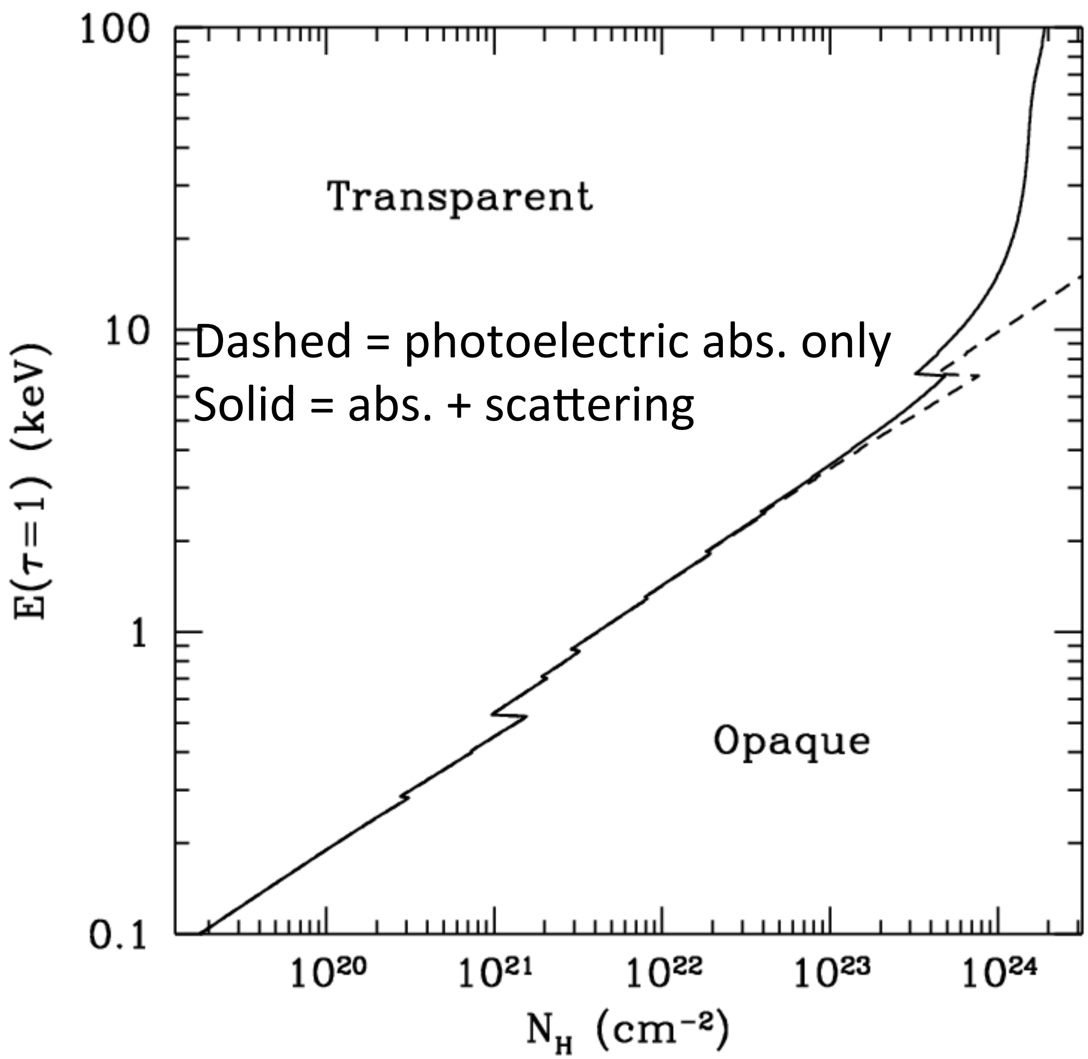

$I_{obs}(E)/I_{int}(E) \approx e^{-\tau}$

$\tau = N_H \sigma$

For $N_H > \sigma_T^{-1} \sim 1.5 \times 10^{24}$ cm^{-2} $\tau_T > 1$

Compton-scattering brings high-E photons to lower E where absorption is effective

➔

medium opaque even at E > 10 keV

These objects are called Compton-thick

AGN X-ray spectral templates with different N_H

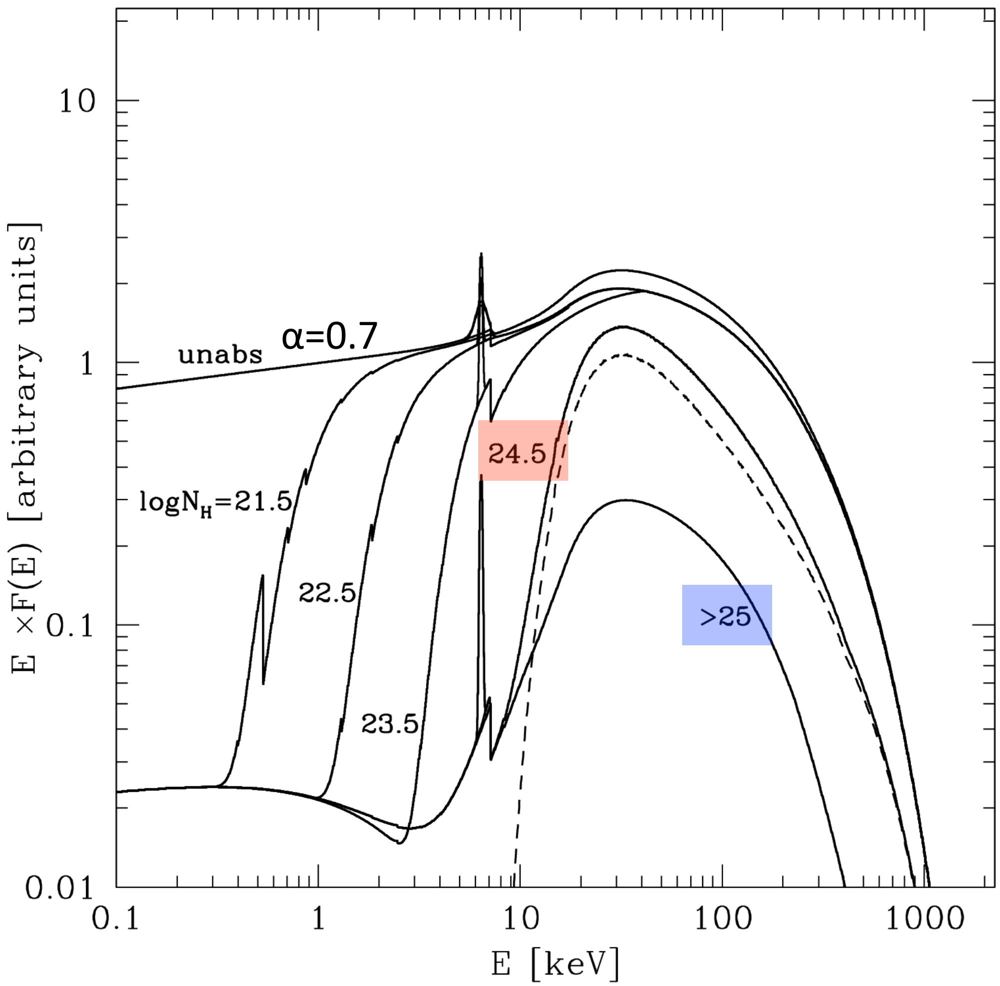

Unabsorbed:
$\log N_H < 21$

Compton-Thin:
$21 < \log N_H < 24$

Compton-Thick:
Mildly ($\log N_H$ =24-25)
Heavily ($\log N_H$ >25)

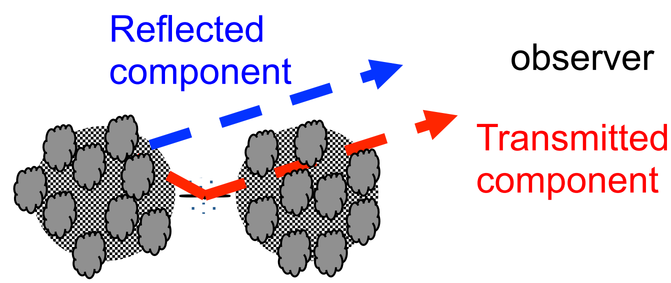

As N_H increases, the spectrum is absorbed towards higher and higher energies.

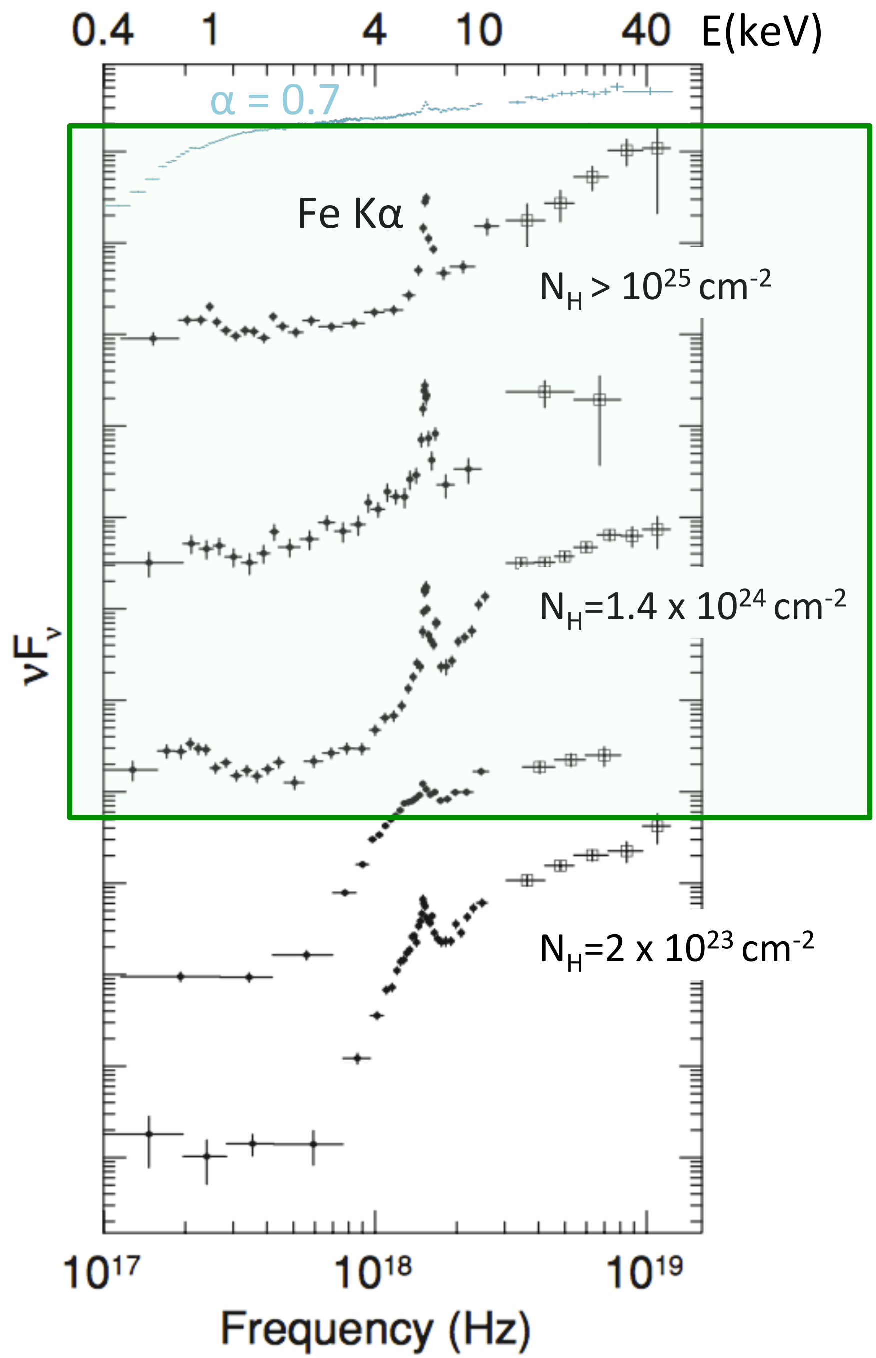

Examples of local Compton-thick AGN

a prominent (EW >~1 keV) Fe Kα line
is the blue print of a Compton-thick nuclei

How abundant are they?

The cosmic X-ray background

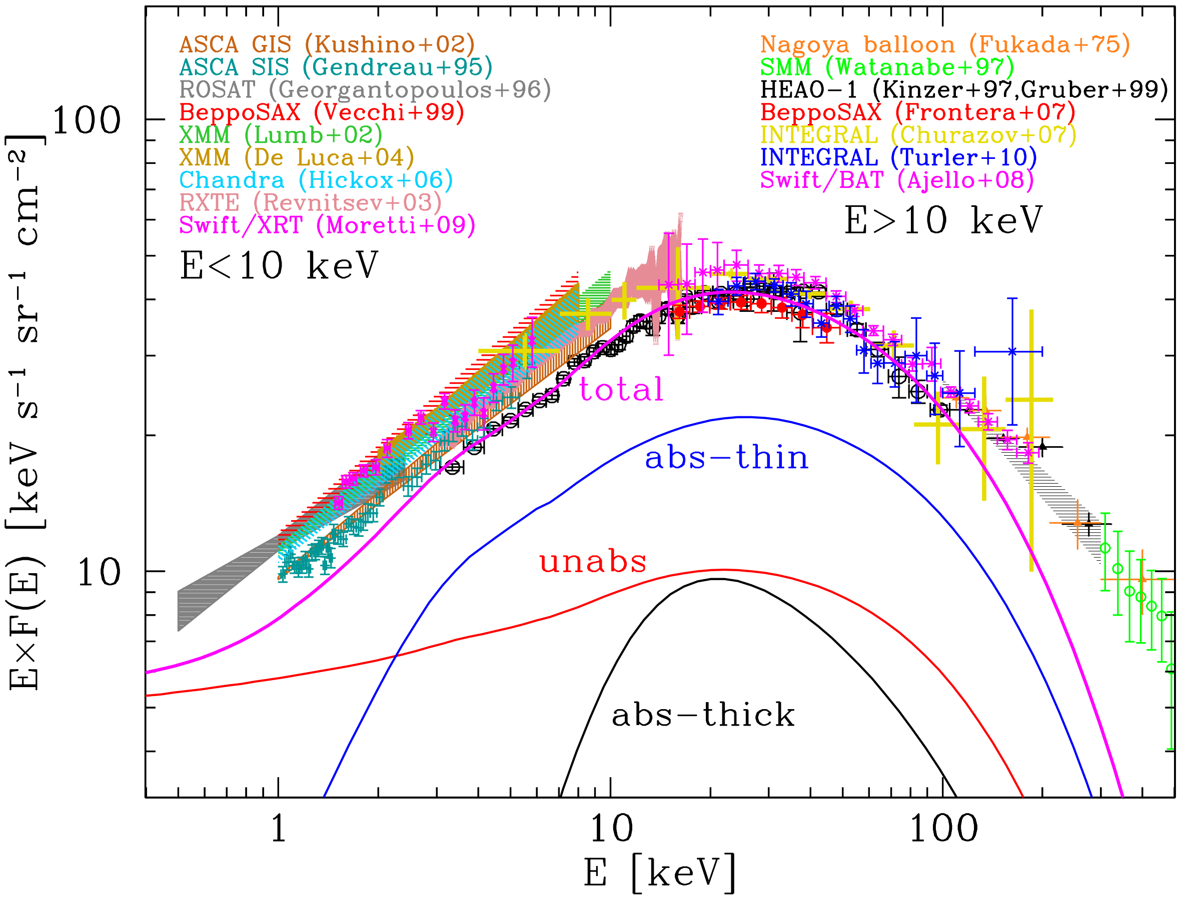

$N_{abs,thin}$ ~ $N_{abs,thick}$ ~ 3 x N_{unabs} ➔

- 80-90% of SMBH growth is obscured
- 40% is heavily obscured (Compton-thick)

at z>6 only unabsorbed QSOs discovered so far
➔ we still miss most of the early SMBH growth

K-correction is favorable for obscured AGN at high-z

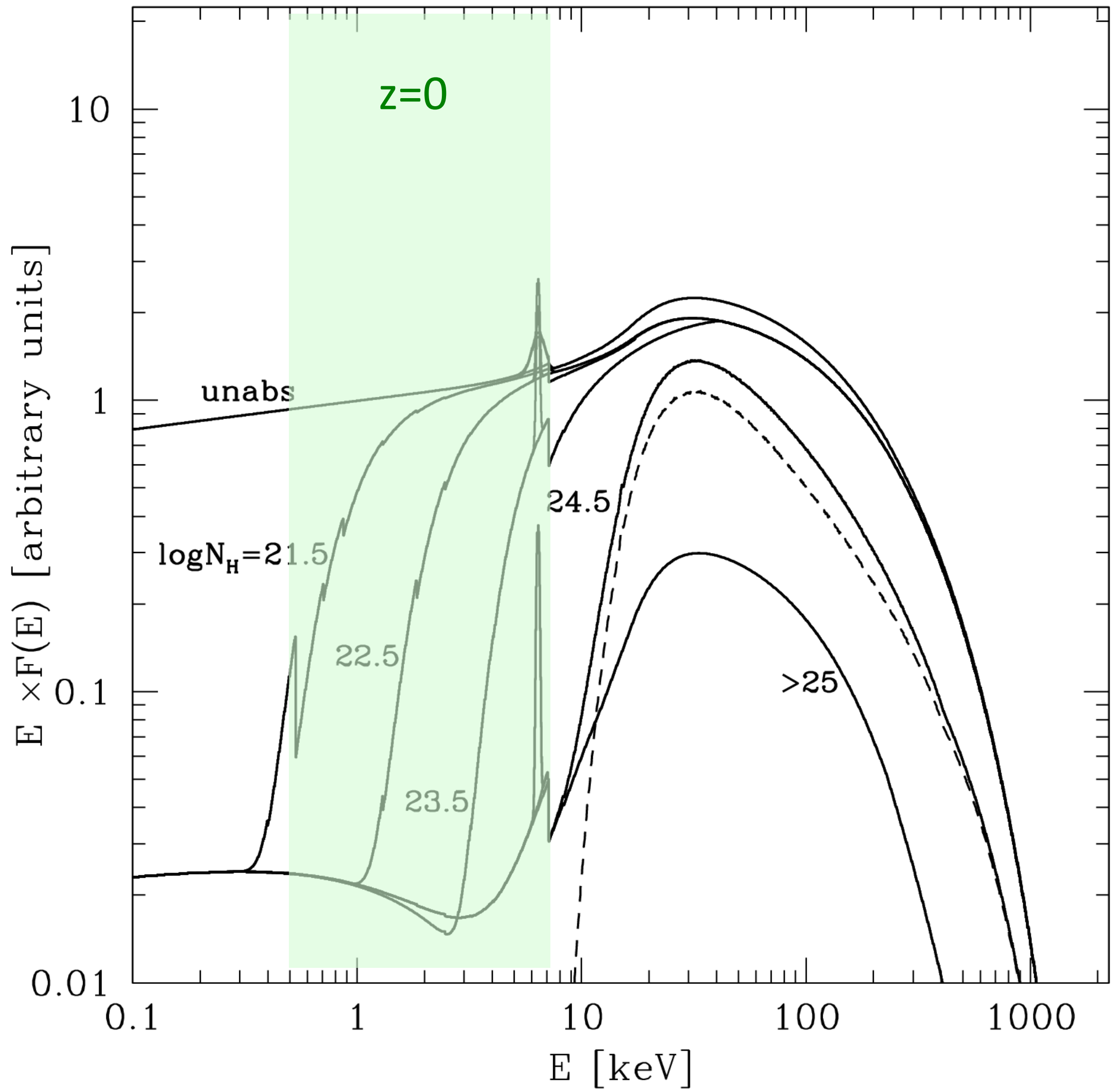

0.5-7 keV rest

Chandra/XMM bandpass

K-correction is favorable for obscured AGN at high-z

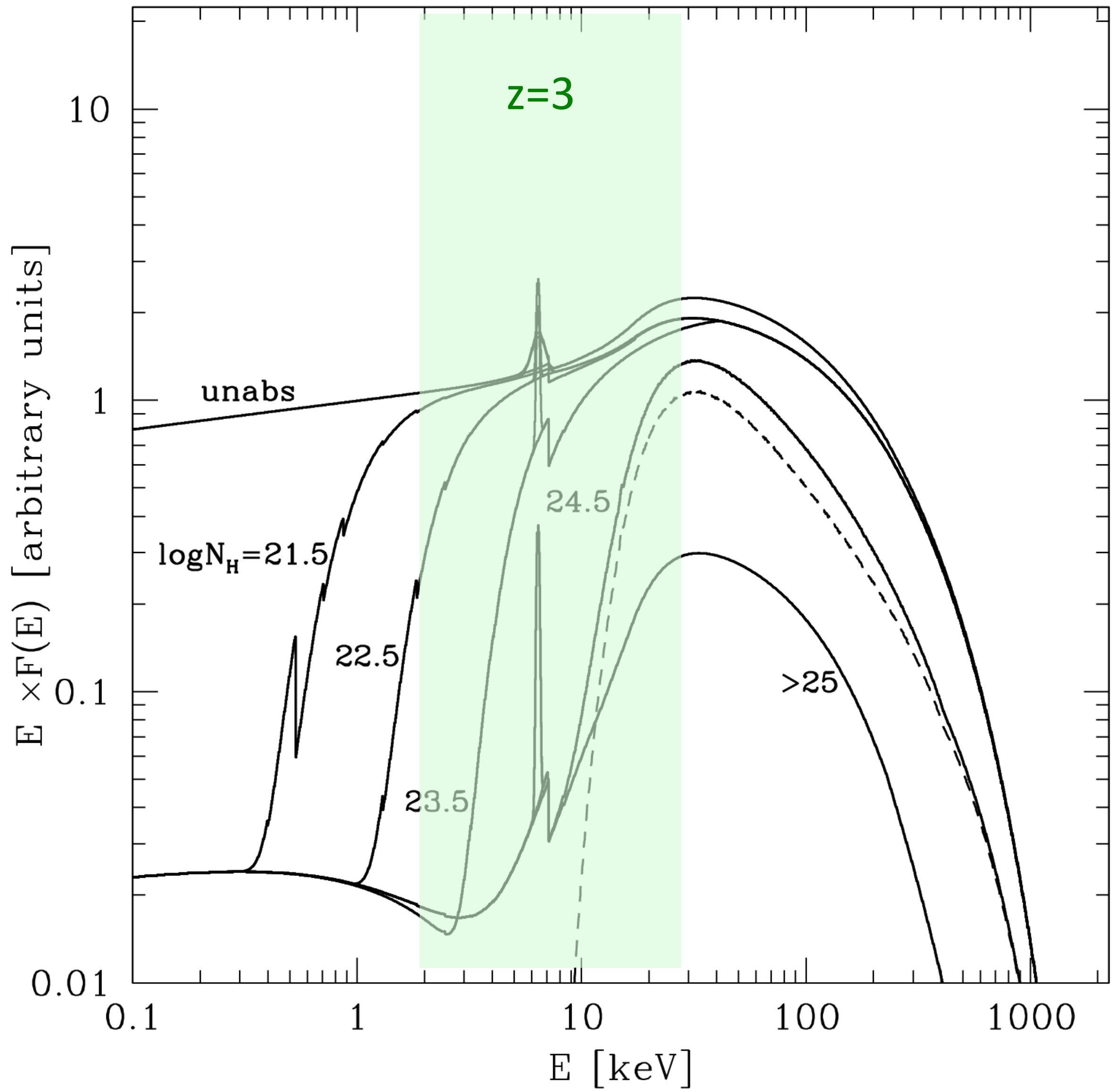

2.0-28 keV rest

K-correction is favorable for obscured AGN at high-z

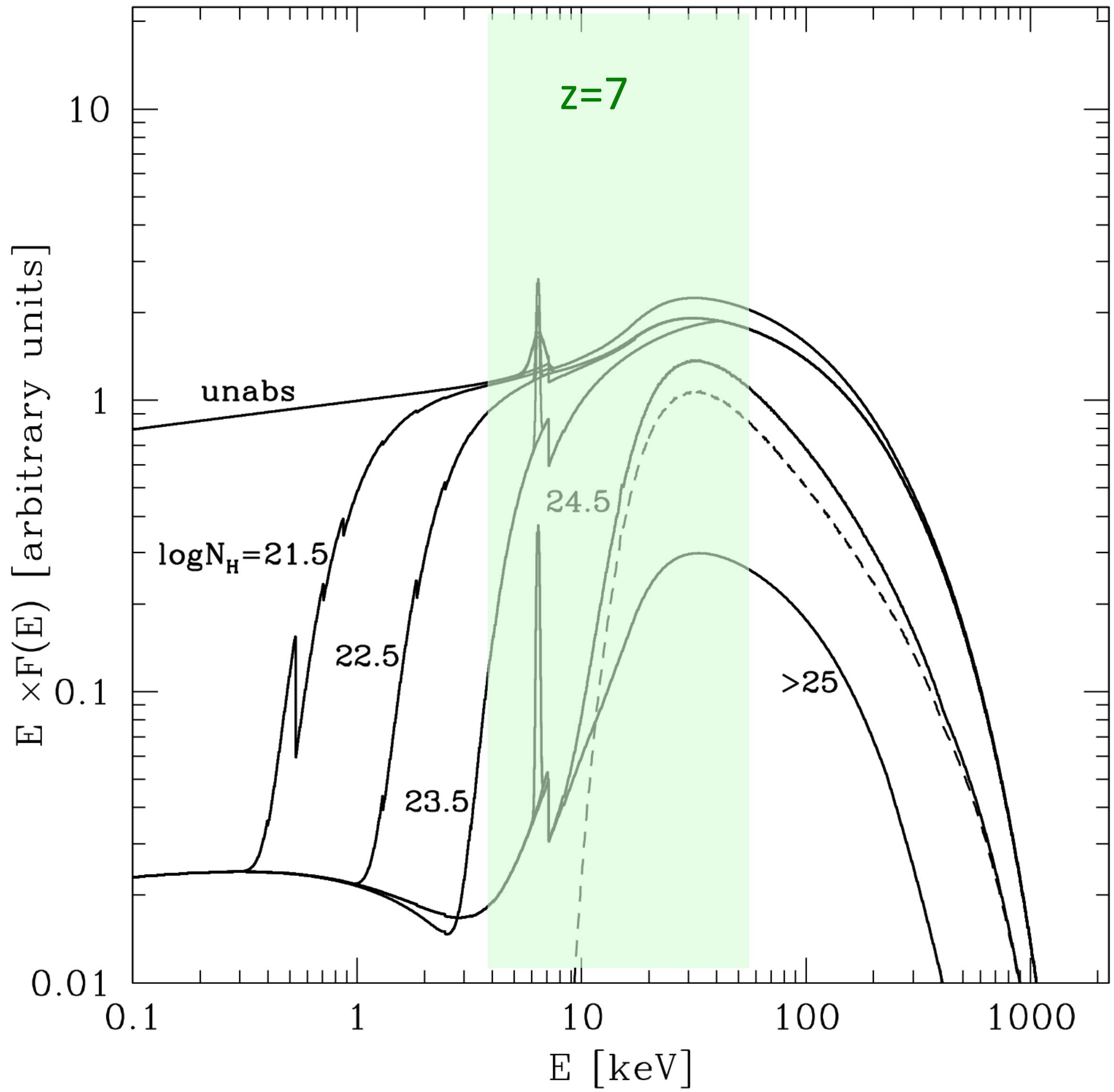

4.0-56 keV rest

$N(E) \sim E^{-2}$

Nonetheless, deep X-ray exposures needed to get good spectra

Extragalactic X-ray surveys

3Ms XMM XXL-South, 23.6 deg^2
Pierre et al. (2015)

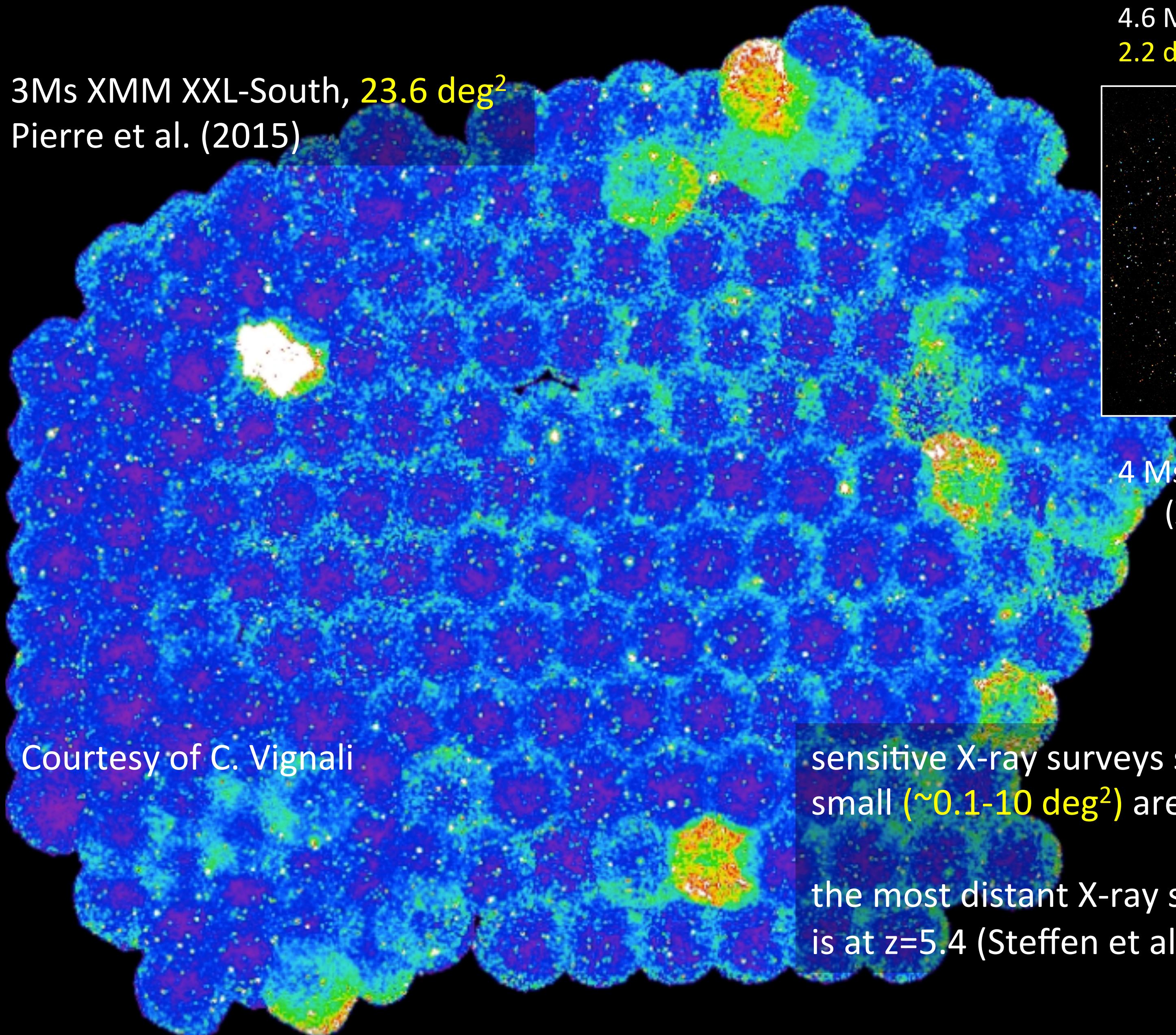

Courtesy of C. Vignali

4.6 Ms COSMOS-Legacy,
2.2 deg^2 (Civano et al. 2015)

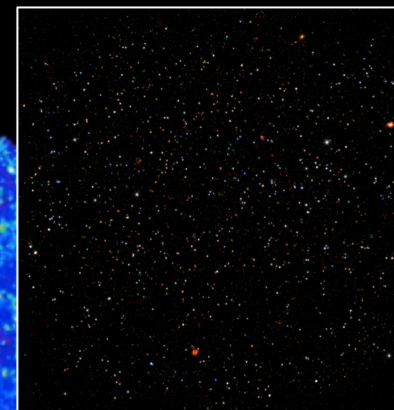

4 Ms CDFS, 0.14 deg^2
(Xue et al. 2011)

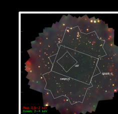

sensitive X-ray surveys still limited to small (~0.1-10 deg^2) areas (see last lecture)

the most distant X-ray selected AGN is at z=5.4 (Steffen et al. 2004)

The deepest X-ray image of the Universe

the 4Ms (1.5 months) Chandra Deep Field South (will reach 7Ms by Dec 2015)

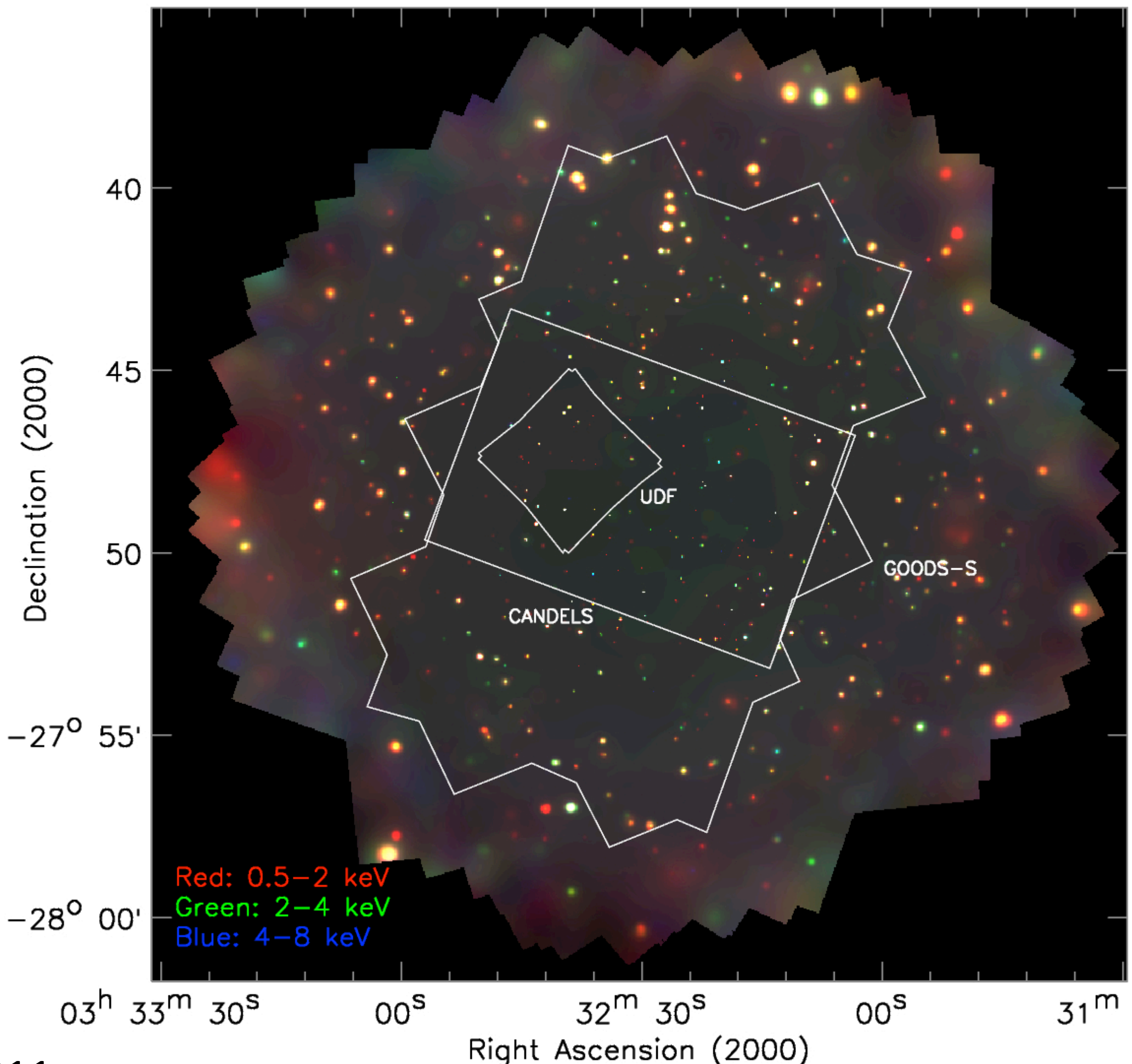

0.14 deg^2

Xue et al. 2011

Examples of X-ray selected AGN at high-z

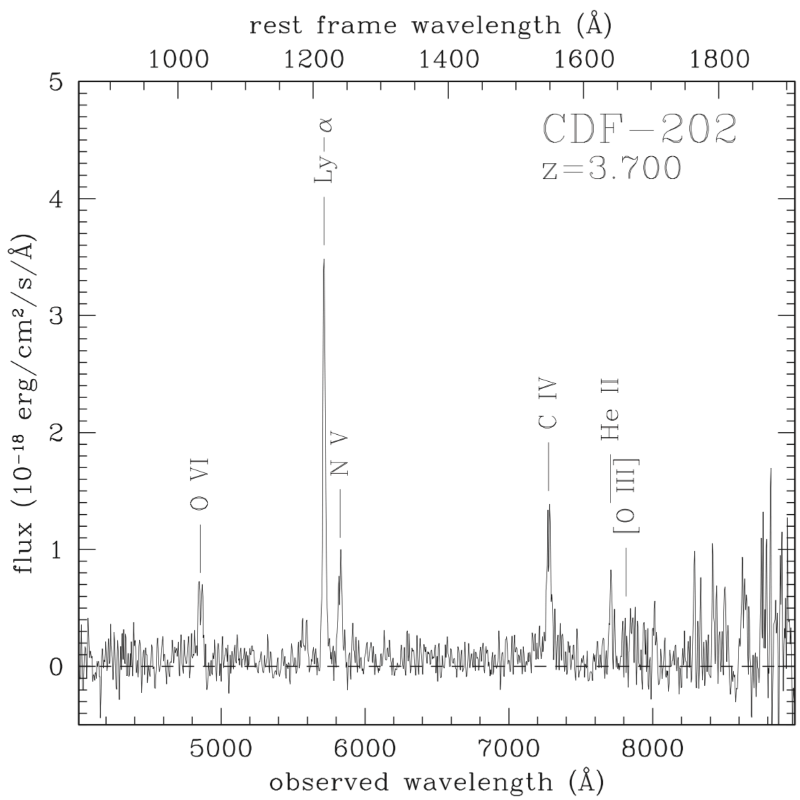

Norman et al. 2002

$N_H = 10^{24}$ cm^{-2}
$L_x = 6 \times 10^{44}$ erg/s

Compton-thick

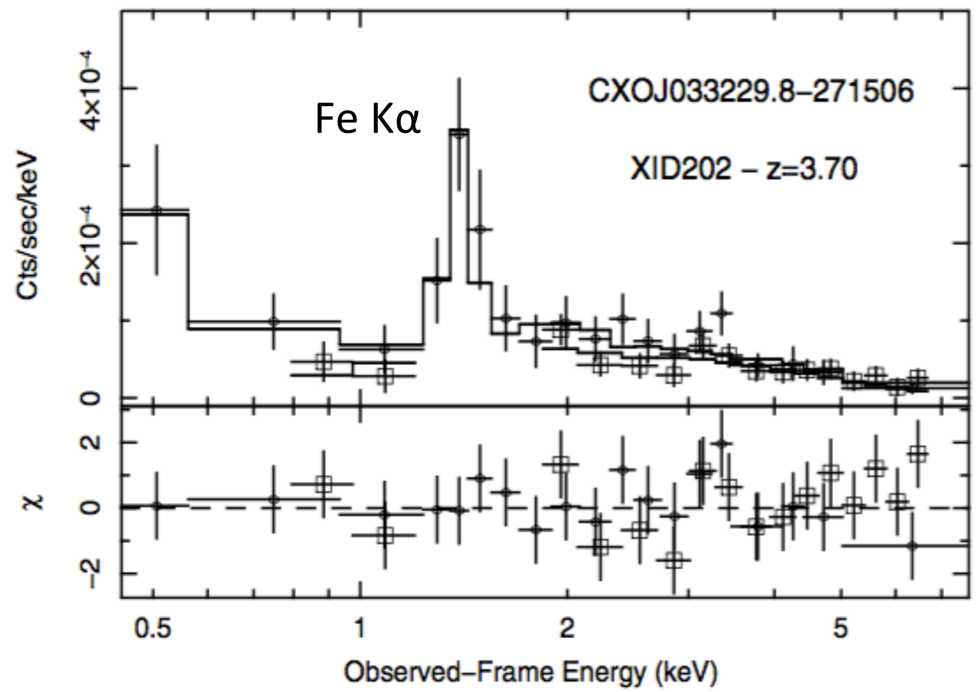

Comastri et al. 2011
(from 3Ms XMM exposure of CDFS)

Examples of X-ray selected AGN at high-z

$N_H = 2 \times 10^{23}$ cm^{-2}
$L_x = 2.5 \times 10^{43}$ erg/s Compton-thin

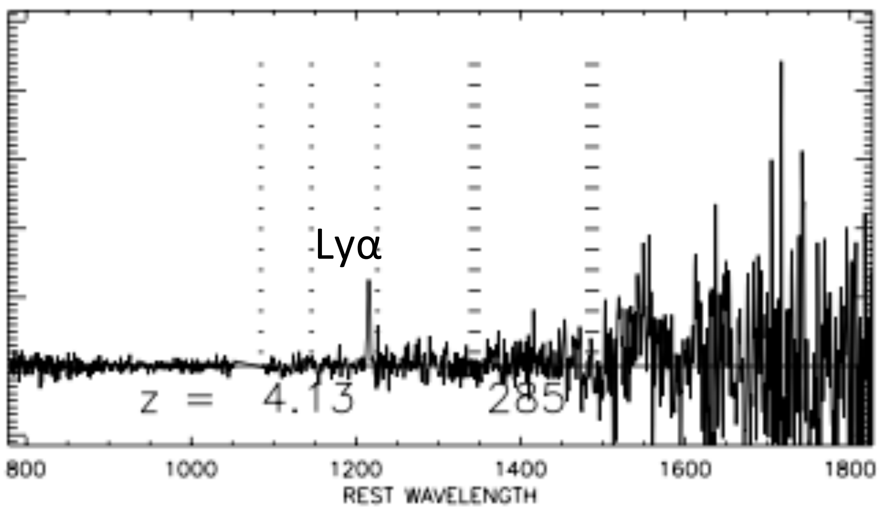

Barger et al. 2002

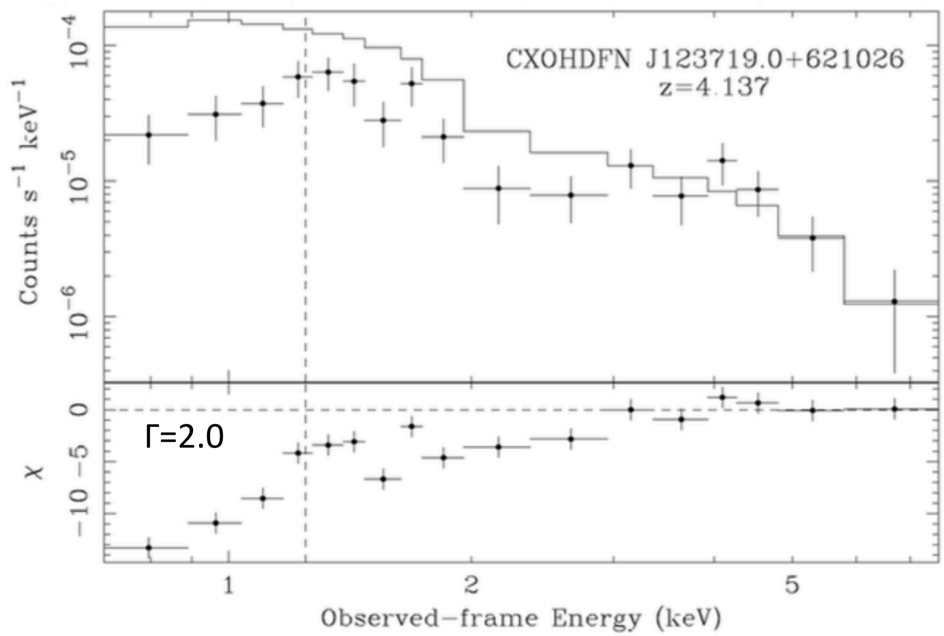

Vignali et al. 2002
(from 2Ms CDFN)

Examples of X-ray selected AGN at high-z

Many candidates rely on photometric redshifts

$N_H < 10^{23}$ cm^{-2}
$L_x = 10^{45}$ erg/s

unobscured

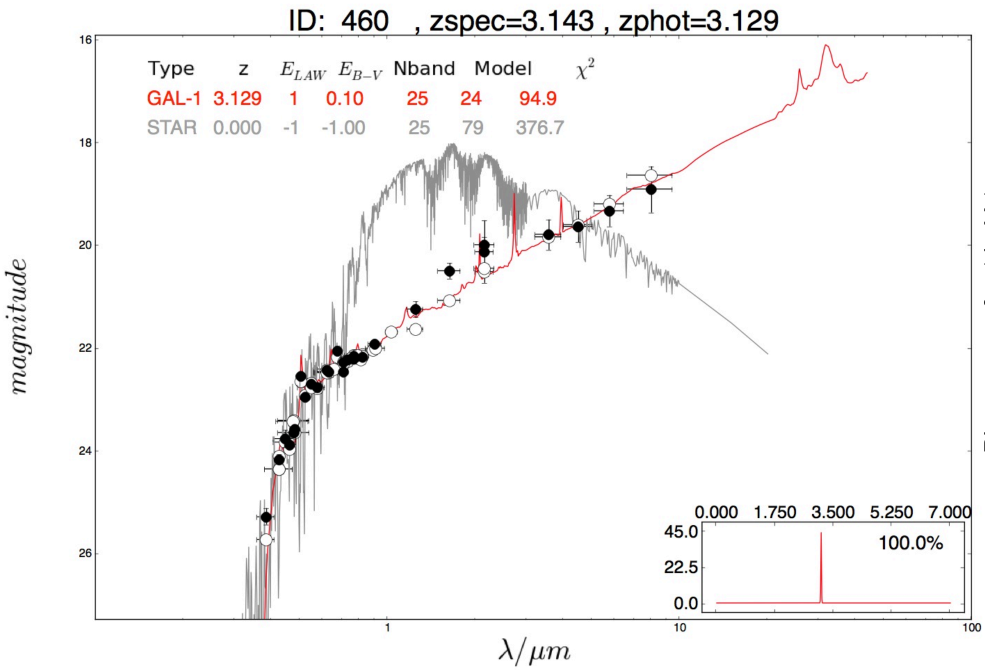

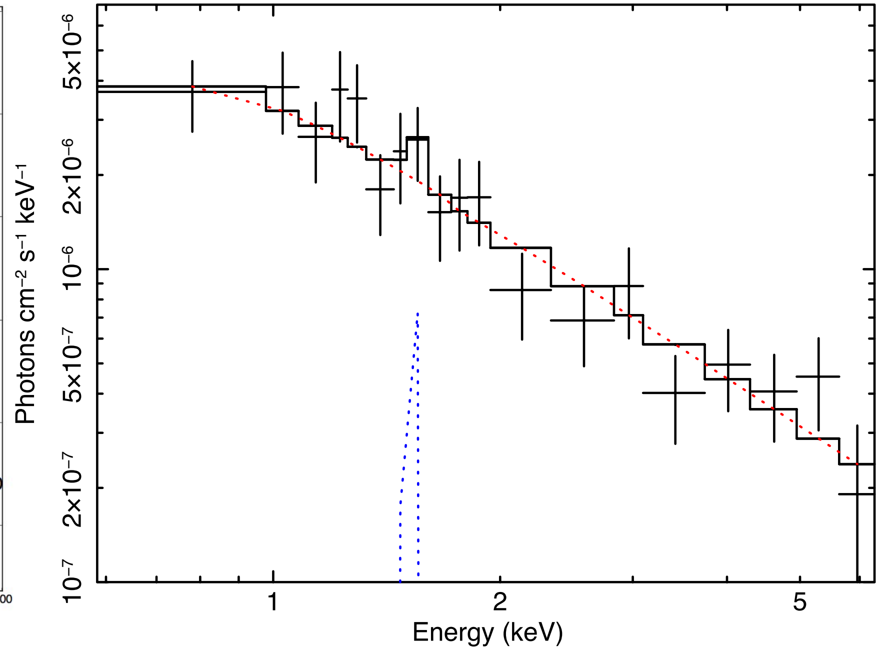

From 4.6 Ms Chandra COSMOS-Legacy

Courtesy of S. Marchesi & G. Lanzuisi

The most distant Compton-thick AGN known to date

LESS 73 = ALESS 73.1 = XID403

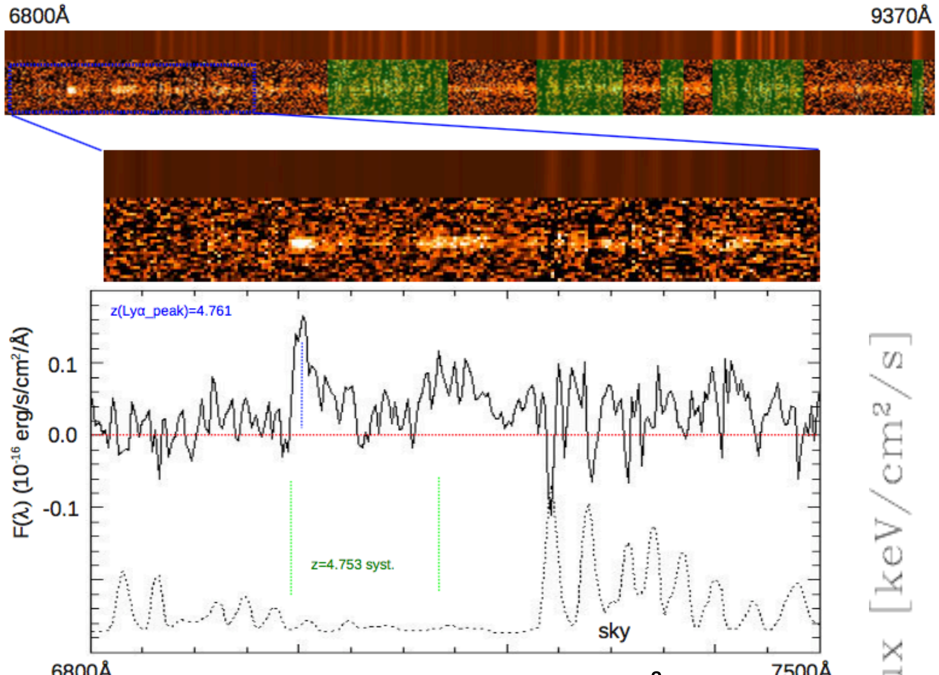

observed wavelength (Å)

z=4.75
(from both optical and submm spectroscopy)

4Ms Chandra spectrum

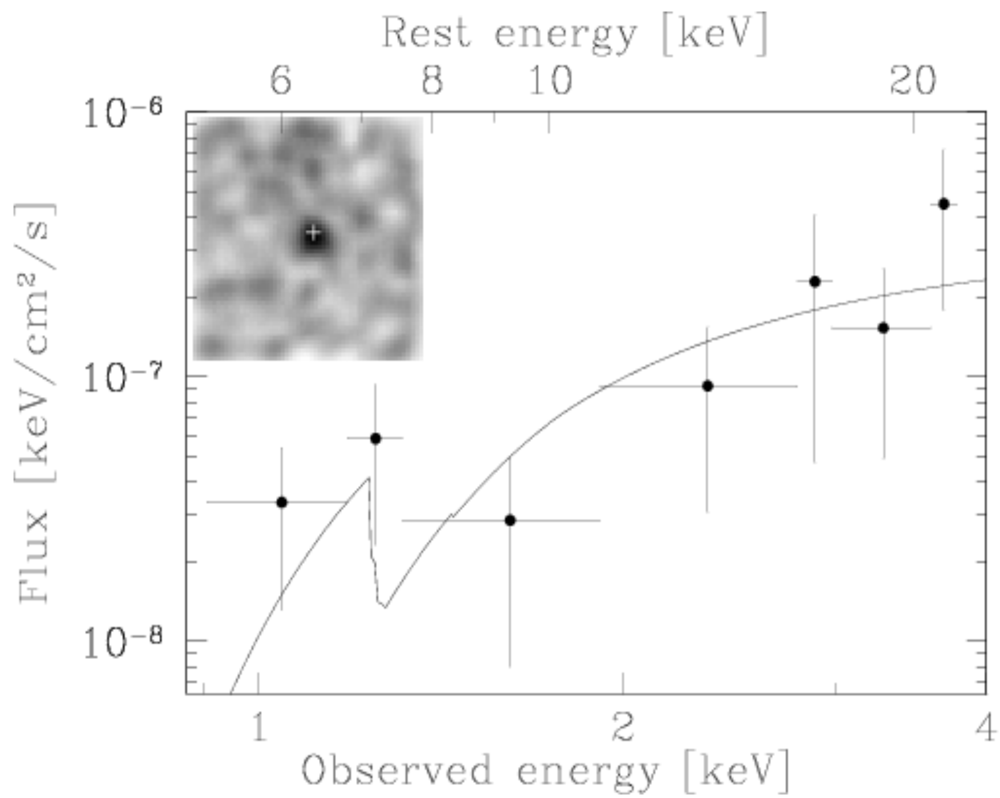

$L_X \sim 2 \times 10^{44}$ erg/s
$N_H \sim 1.4\ 10^{24}$ cm^{-2} → Compton-thick QSO

FIR and broad band SED

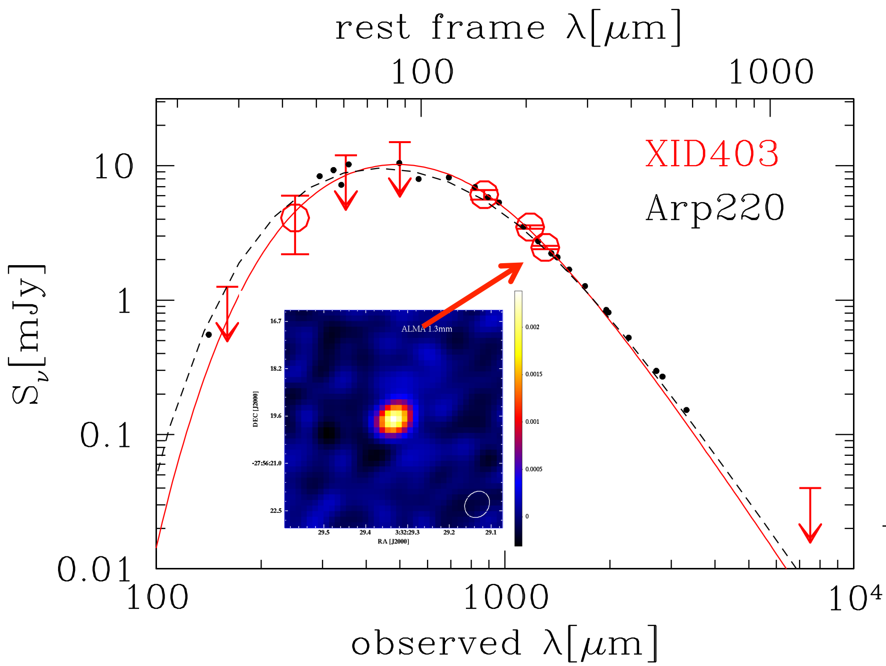

M_{dust} = 4.9 (± 0.7) x 10^8 M_{sun}

$r_{50\%,dust}$ ~ 0.9 (± 0.3) kpc (0.3" or less)

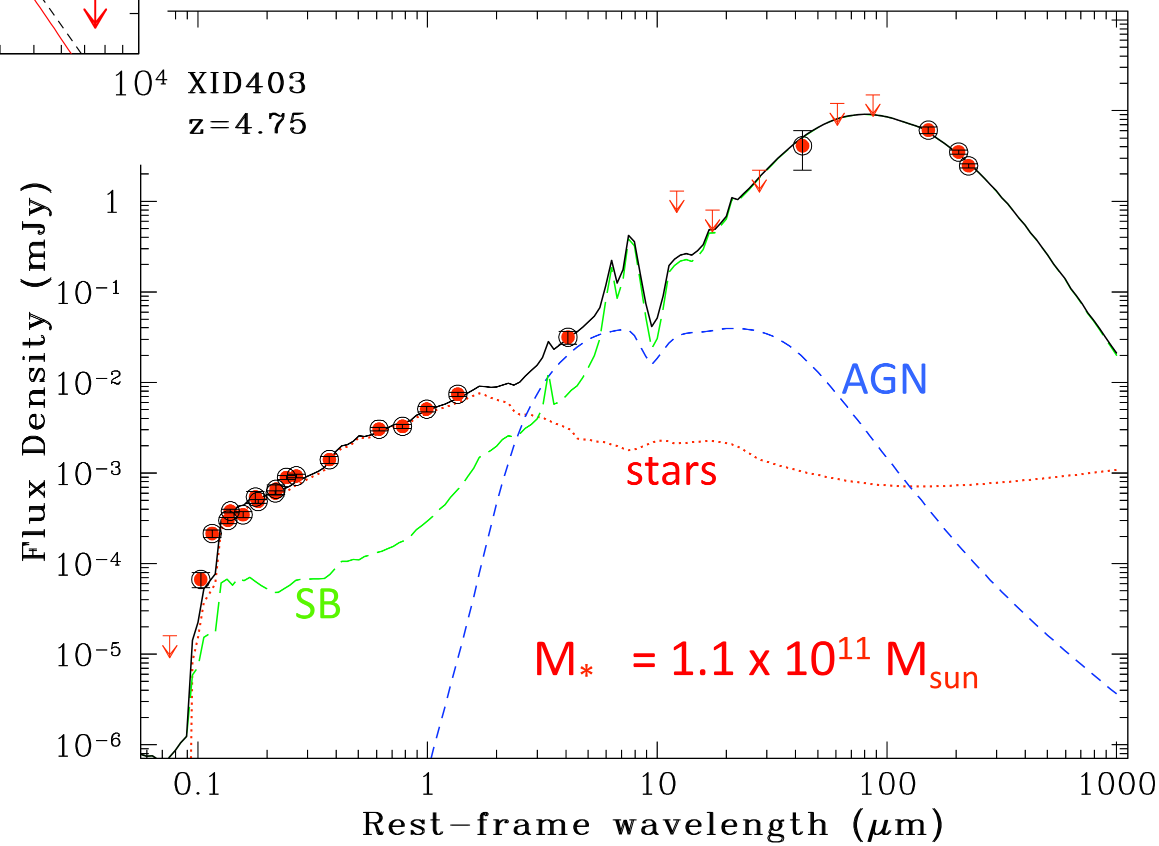

M_{HI+H_2} ~ 2x10^{10} M_{sun}
(De Breuck et al. 2014)

If gas and dust co-spatial:
N_{HI+H_2} = 0.3-1.1 x 10^{24} cm^2
comparable with X-rays

→obscuration by host ISM?
Z = Z_{sun} (Nagao et al. 2012)

Dynamical mass

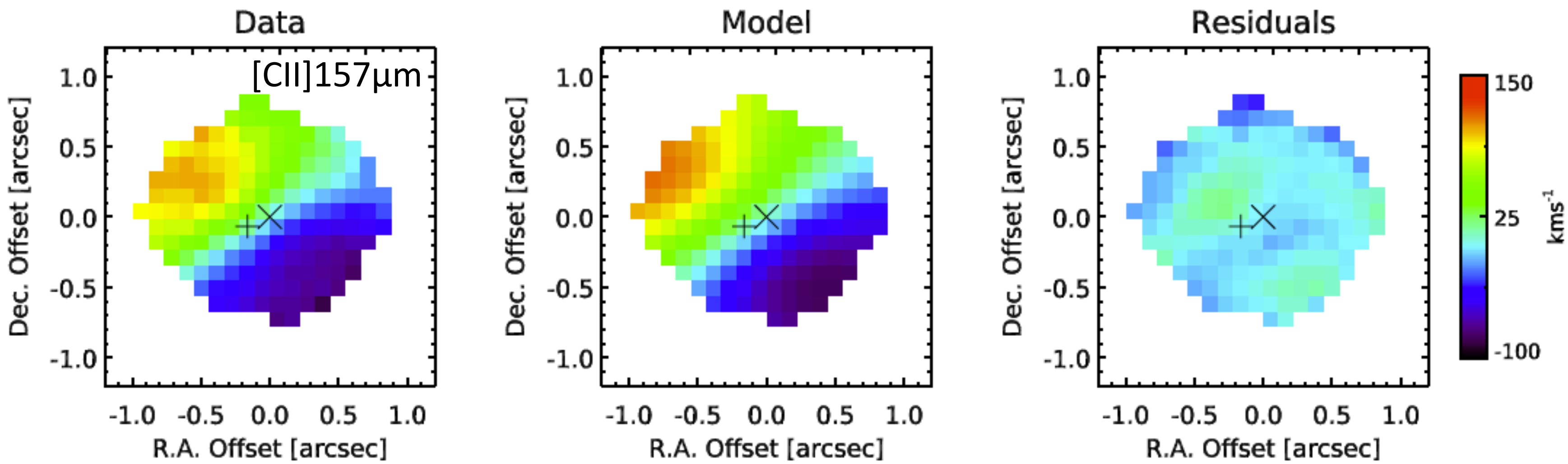

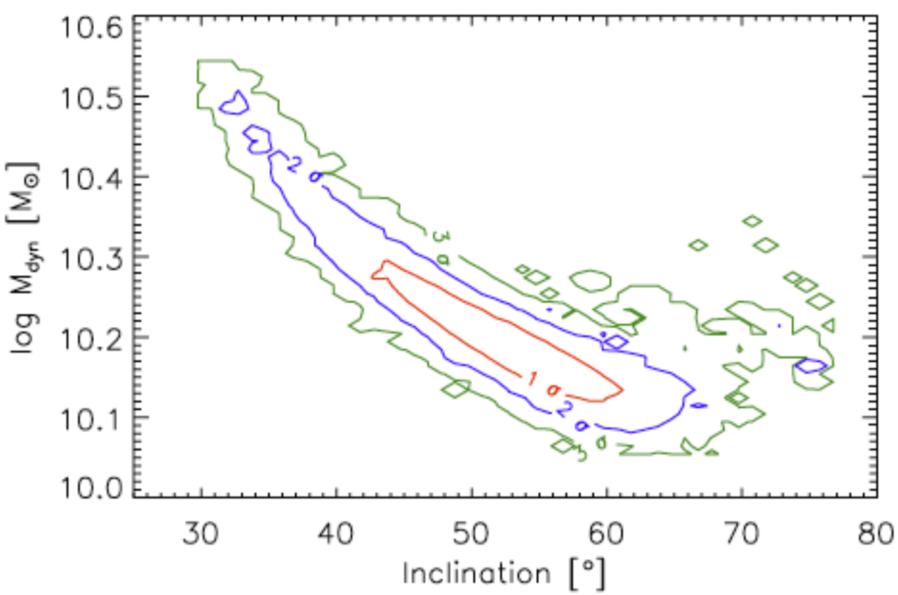

De Breuck et al. 2014 (1.6hr ALMA)

M_{dyn} = 3x10^{10} M_{sun}

M_* = 1x10^{10} M_{sun}
(1 dex smaller than from SED fitting!)

Dust and stellar mass

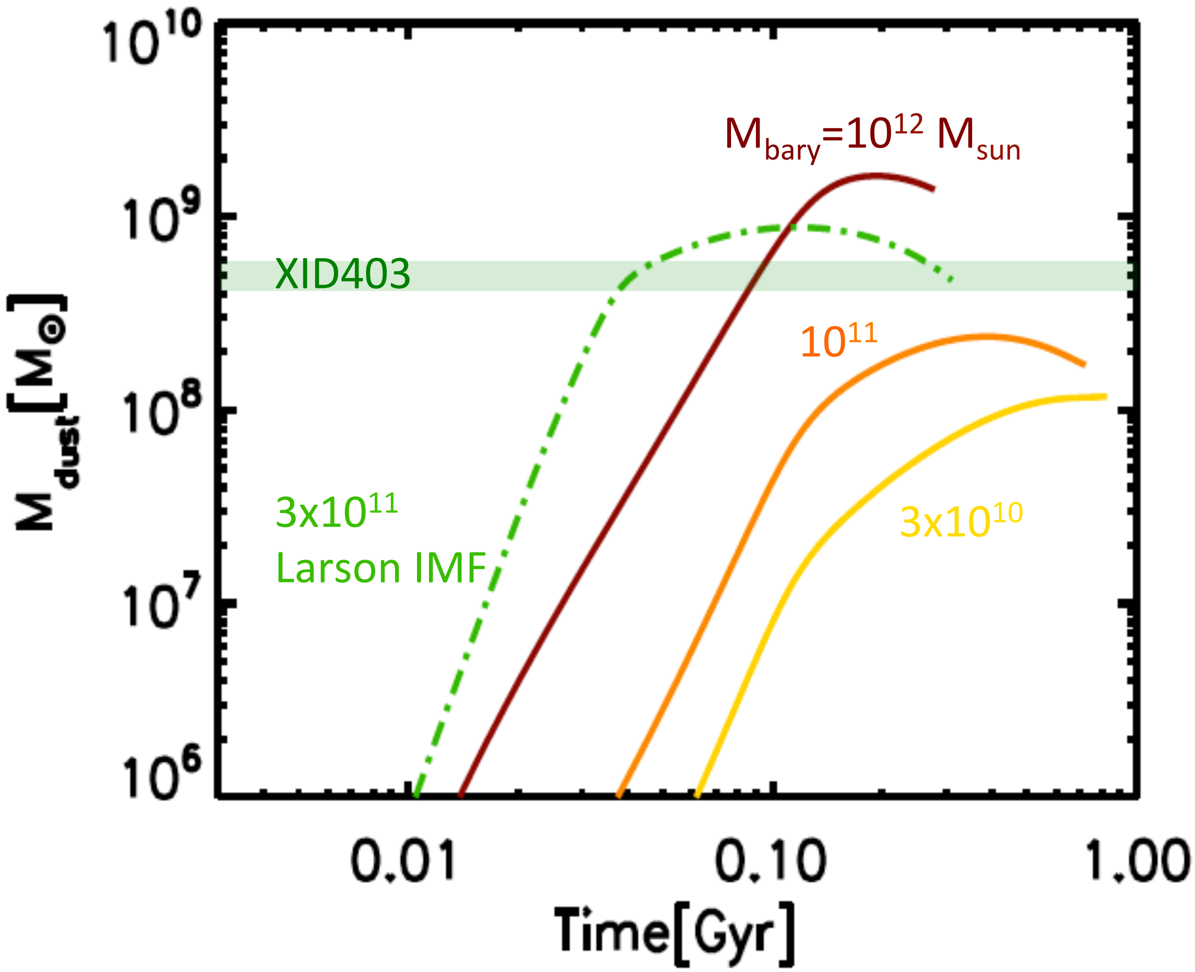

Calura et al. 2014

M_{dust} is ok with M_* from SED-fitting

again, tension between M_{dust} (and M_*) vs M_{dyn} , as for z~6 QSOs

The X-ray luminosity function

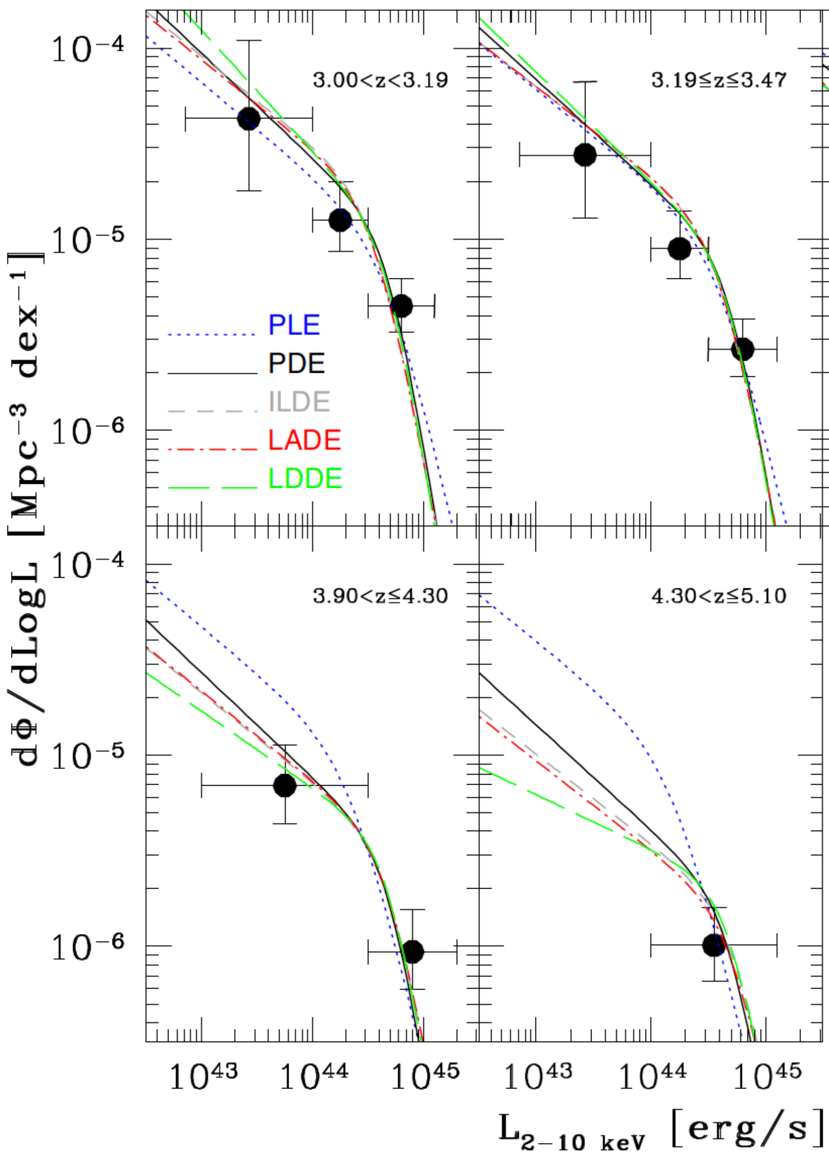

Vito et al. 2014

see also Kalfountzou et al. 2014, Georgakakis et al. 2015

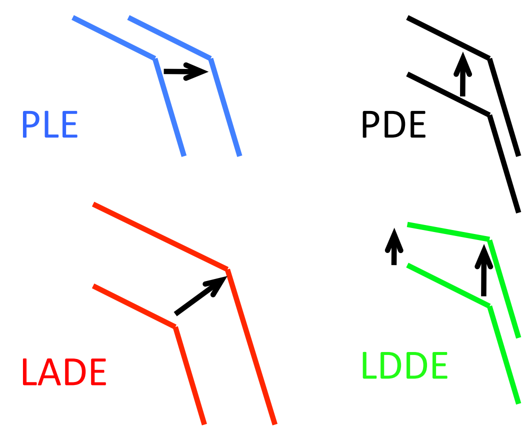

limit of current AGN XLFs: $\log L_x > 44$ at $z > 4$

($L_{bol} > 10^{12}\ L_{sun}$ ➔ $M_{BH} > 3 \times 10^7\ \lambda_{Edd}^{-1}\ M_{sun}$)

Space density of X-ray AGN at z>3

141 AGN (obscured+unobscured)
at z>3 in deep X-ray fields
55% spec-z, 45% phot-z

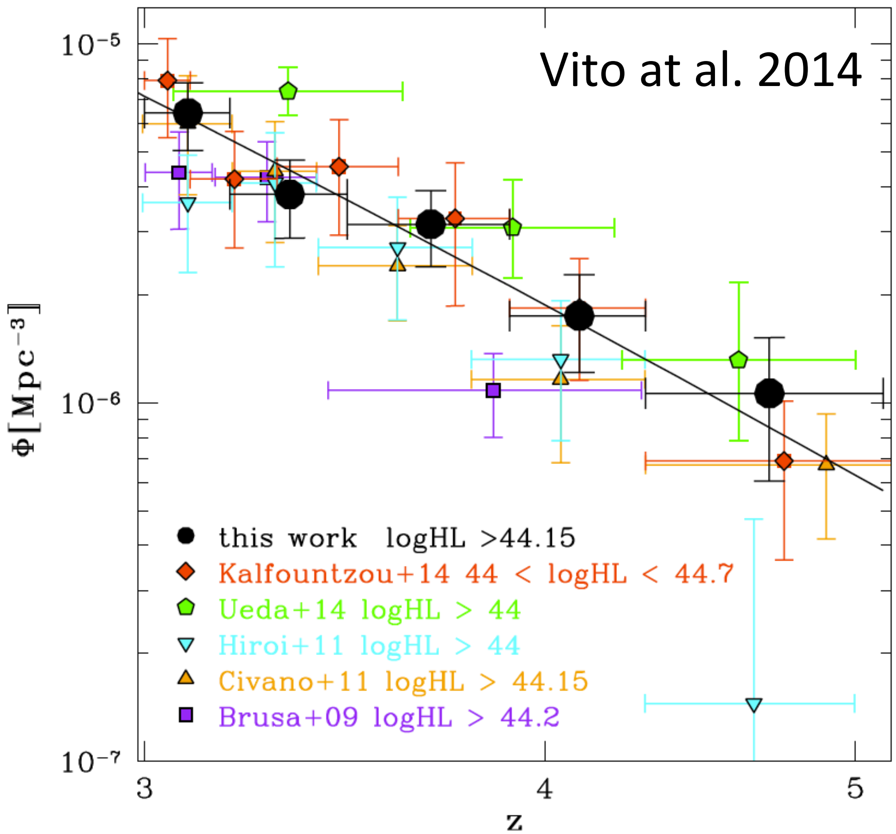

$\phi(z) \sim (1+z)^{-6}$ ➔

~1 dex decrease from z=3 to z=5

exactly like brighter SDSS QSOs

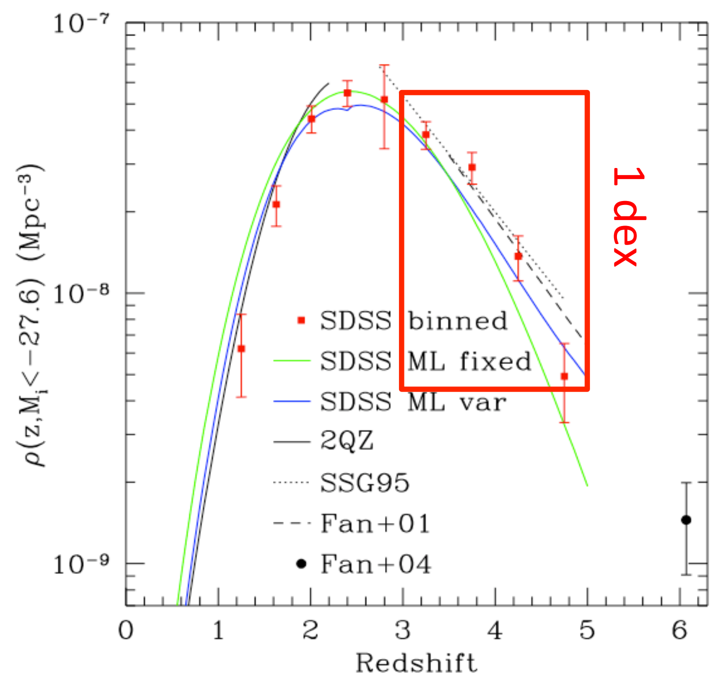

Obscured AGN fraction at z>3

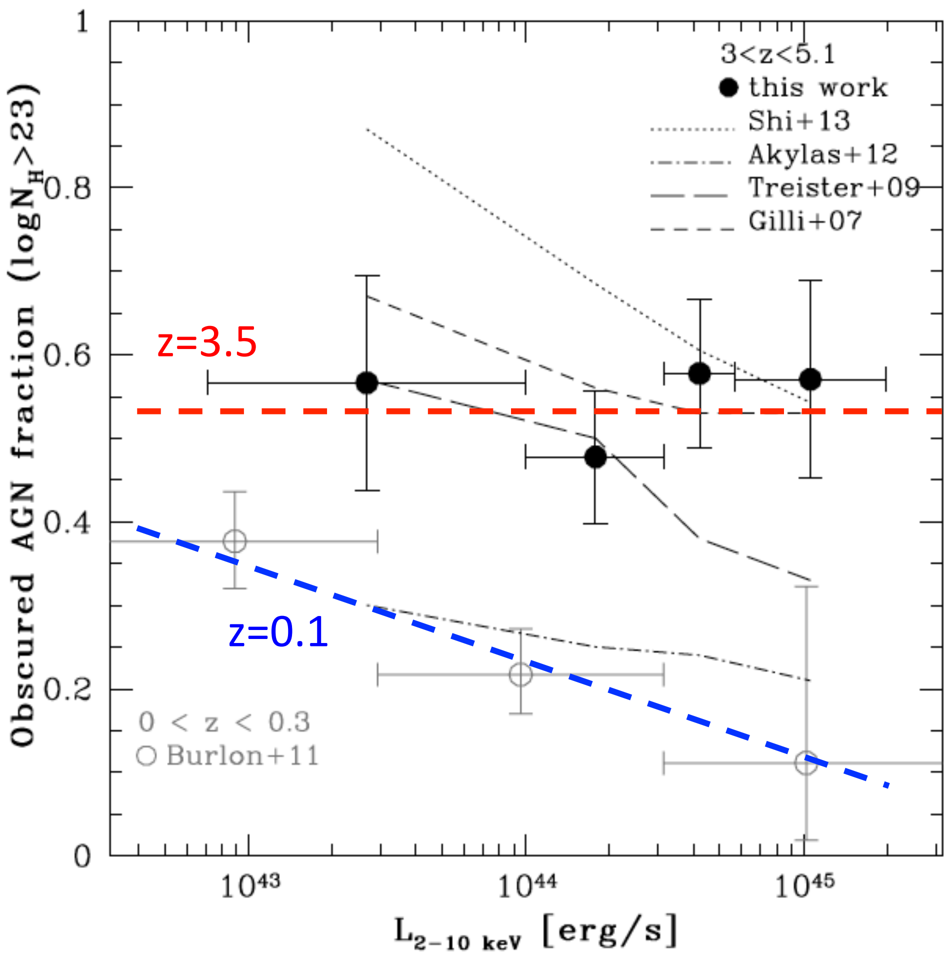

The fraction of luminous obscured AGN increases significantly with redshift (La Franca et al. 2005, Treister et al. 2006, Ueda et al. 2014, ...)

Half of z>3 AGN are obscured by $\log N_H > 23$

Possibly due to higher gas fraction and merger rate at high-z?
(Menci et al. 2008, Lamastra et al. 2010)
Increasing absorption contribution from host ISM, as in XID403?

Vito et al. 2014

Pushing AGN detection to the faintest limits

X-ray photometry at the position of optical dropouts in CANDELS

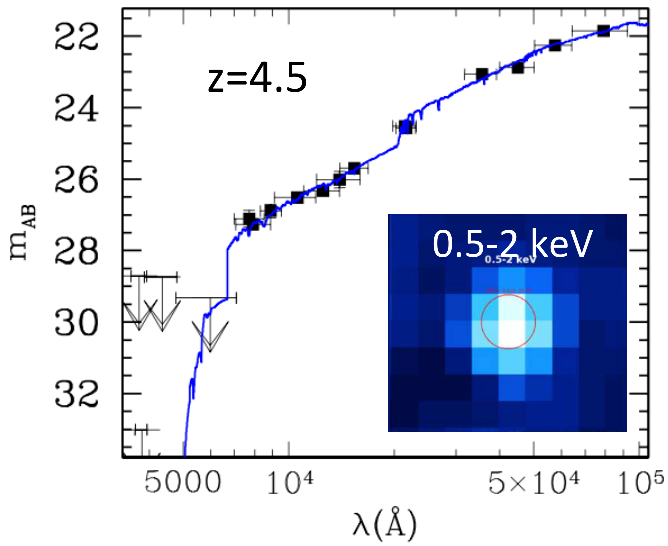

$\log L_x$ = 42.6 – 44 at z > 4

$M_{BH} > 10^6 \lambda_{Edd}^{-1} M_{sun}$

Giallongo et al. 2015

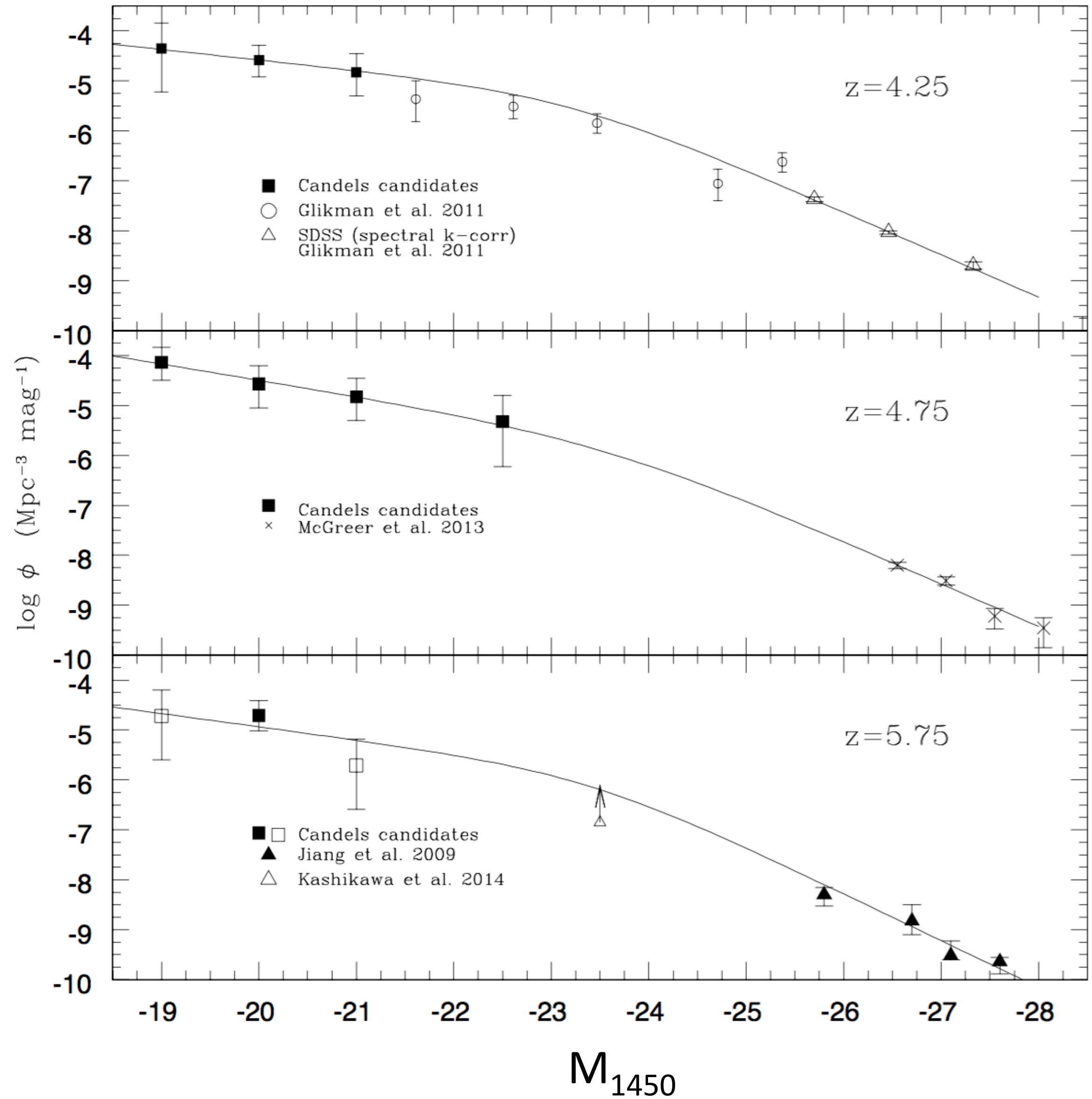

AGN contribution to cosmic reionization

ε_{ion} = AGN hydrogen ionizing emissivity
$\langle f \rangle = L_{esc}/L_{int}$ @ 912Å = escape fraction
ε_{912} = total emissivity at the Lyman limit

$$\epsilon_{ion}(z) = \langle f \rangle \epsilon_{912} =$$
$$\langle f \rangle \int \phi(L_{1450}, z) L_{1450} \left(\frac{1200}{1450}\right)^{0.44} \left(\frac{912}{1200}\right)^{1.57} dL_{1450}$$

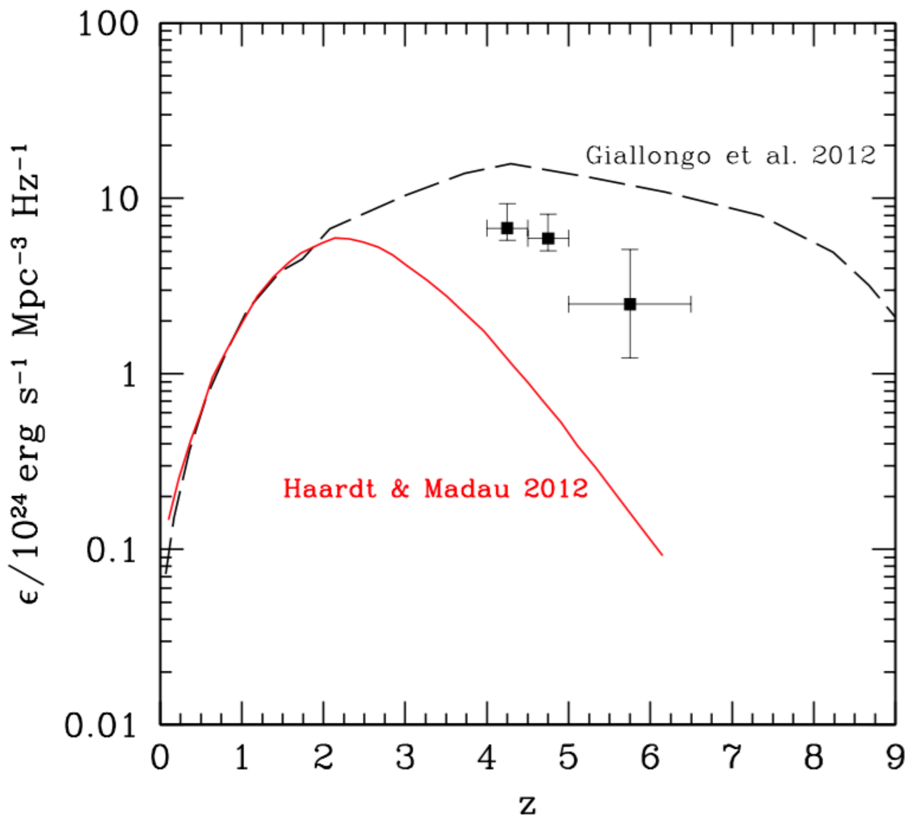

Rate of ionizing photons per H atom

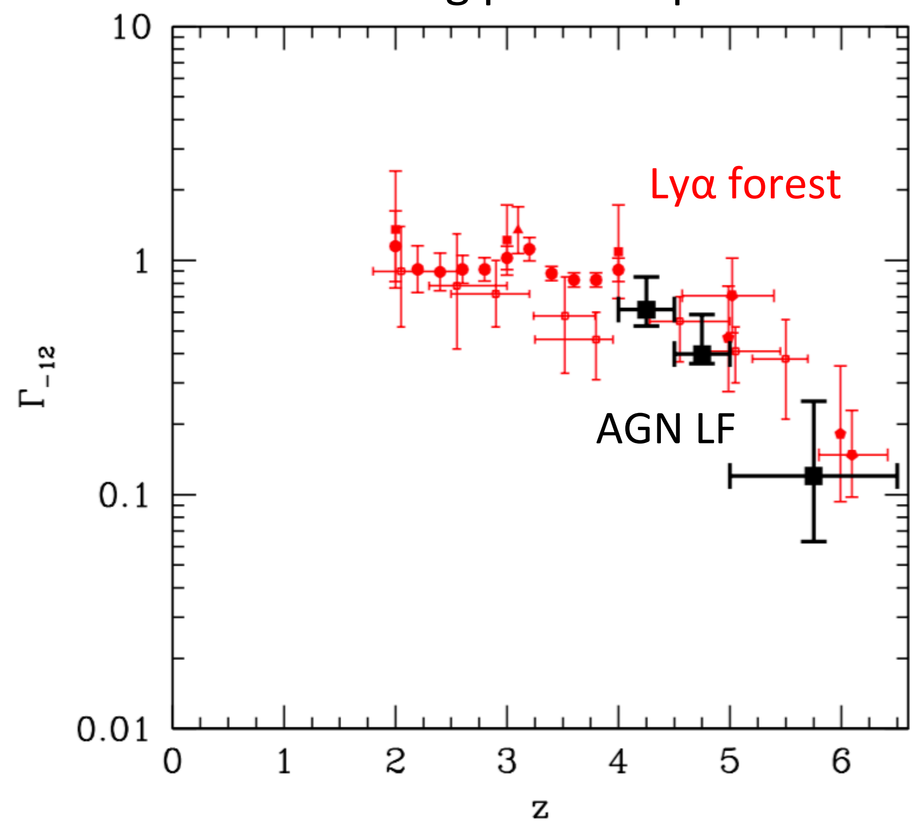

AGN can provide a significant contribution to cosmic reionization (provided f_{esc}~1)
Is this reasonable? See lectures by E. Vanzella

z>3 AGN in the CDFS

L_x ~ a few x 10^{44} erg/s

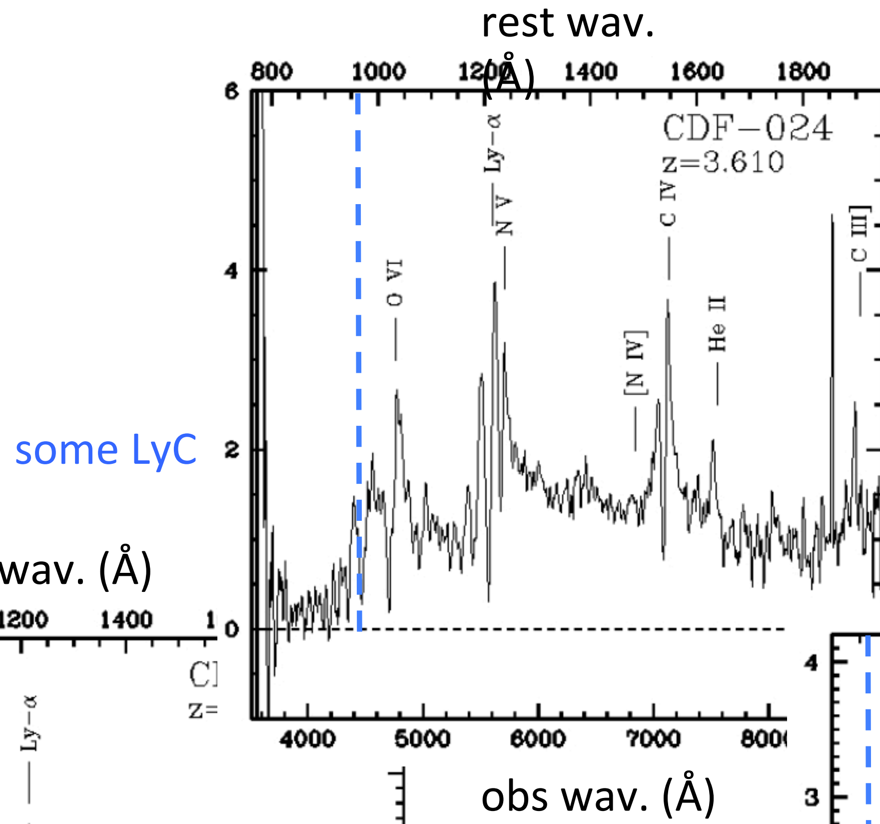

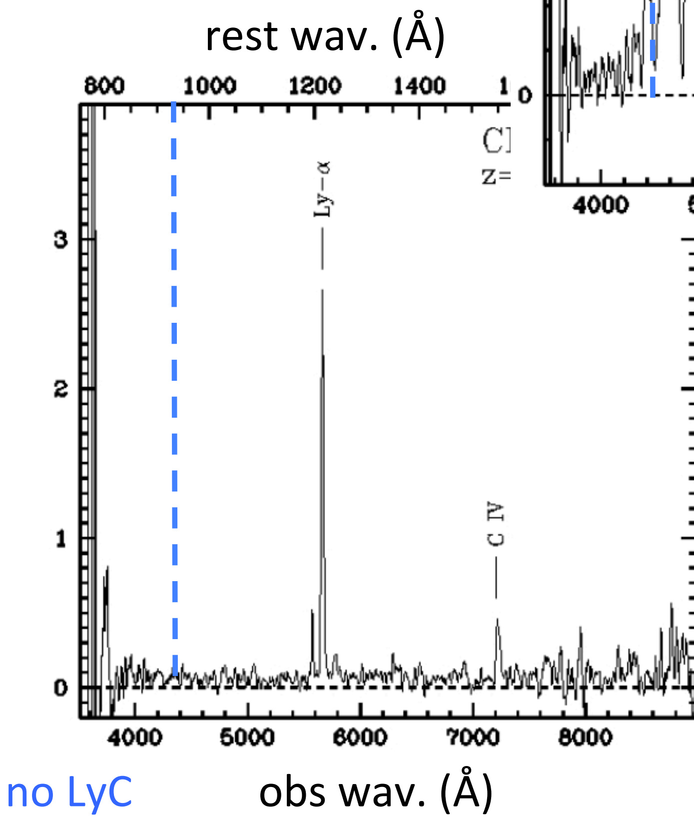

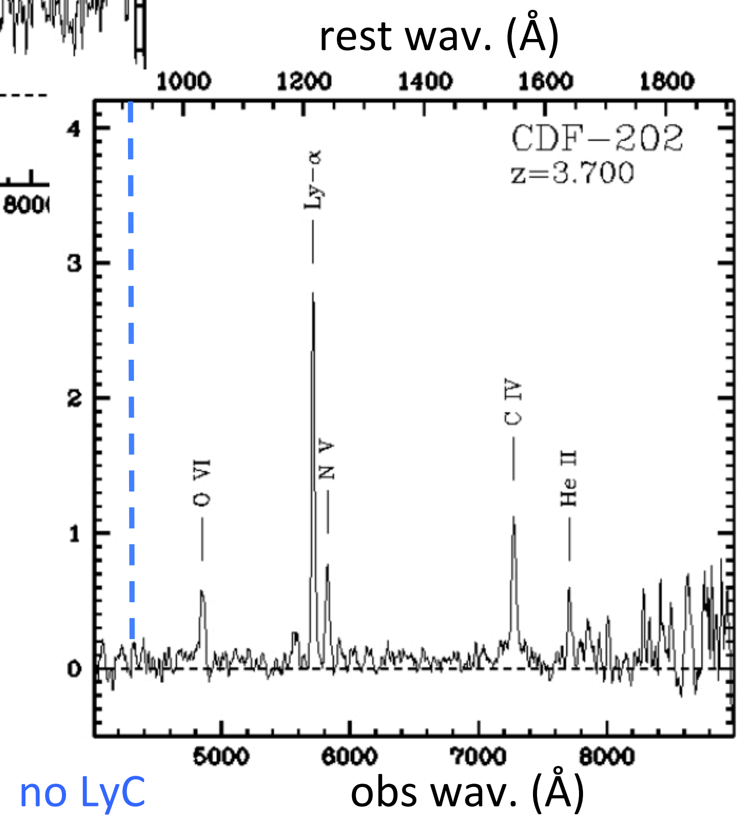

Pushing AGN detection to the faintest limits

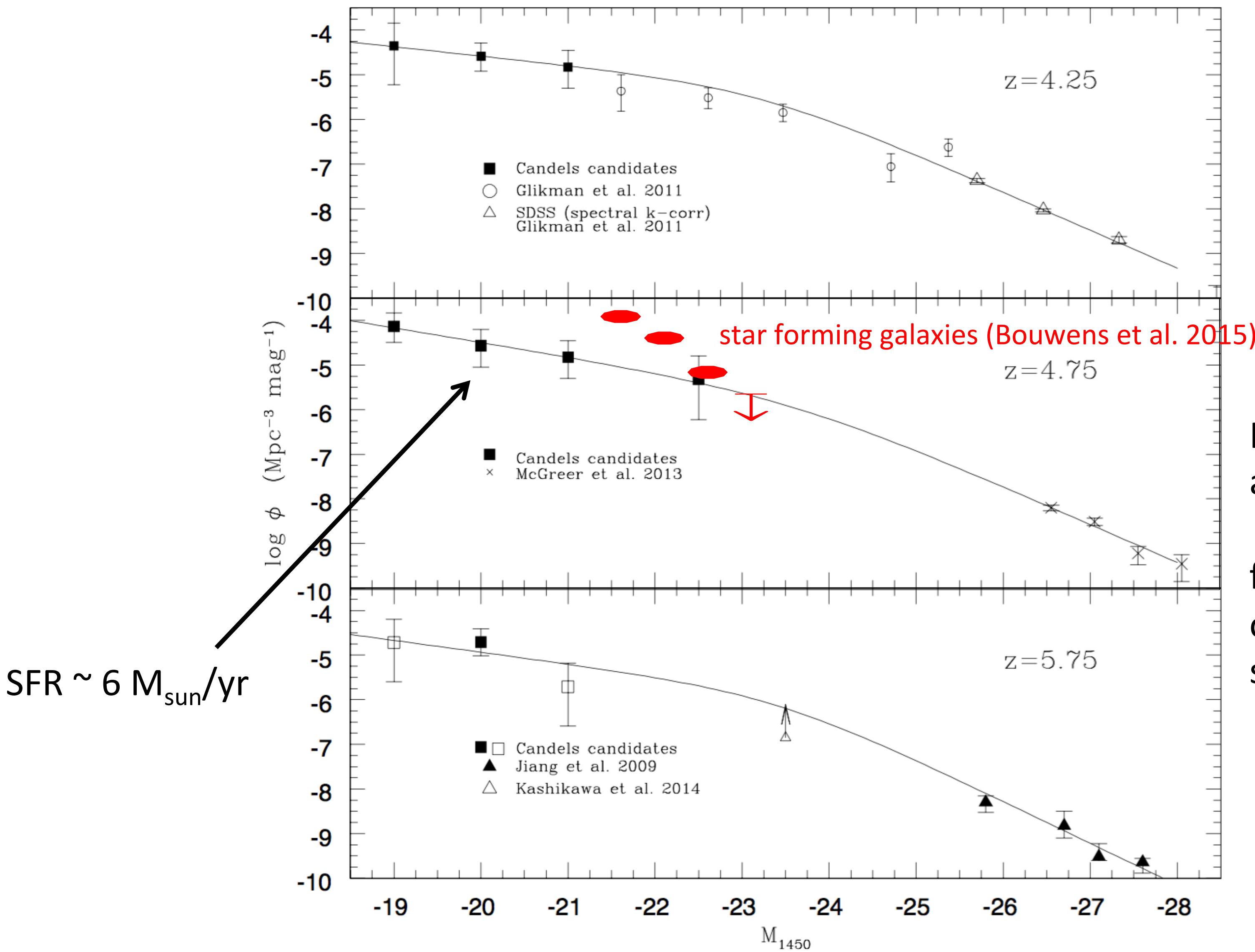

How many are real AGN?

faint end of the AGN LF still uncertain

Pushing even beyond individual detections: cosmic backgrounds

X-ray background fluctuations correlate with near-IR bkg fluctuations at >3µm
but NOT with
optical bkg fluctuations
➔
population of X-ray emitting IR dropouts
➔
high-z (z>7) accreting BHs

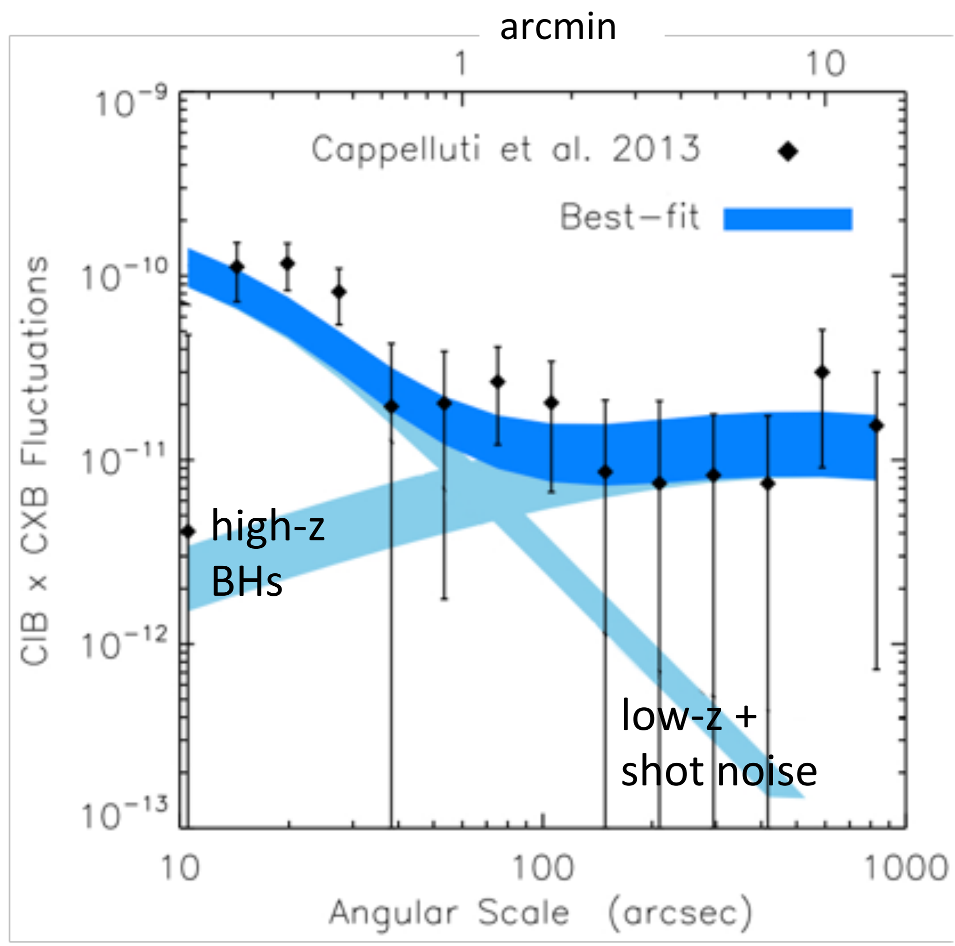

Helgason et al. 2014

Background fluctuations from Direct Collapse Black Holes?

DCBHs (10^4-10^6 M_{sun})

ρ_{DCBH} = mass density of DCBHs

$\rho_{BH,local}$ = mass density of local SMBHs

$\rho_{DCBH} > \rho_{BH,local}$ →

at z=0
there should be 100-1000 dormant DCBHs per galaxy:
too many?

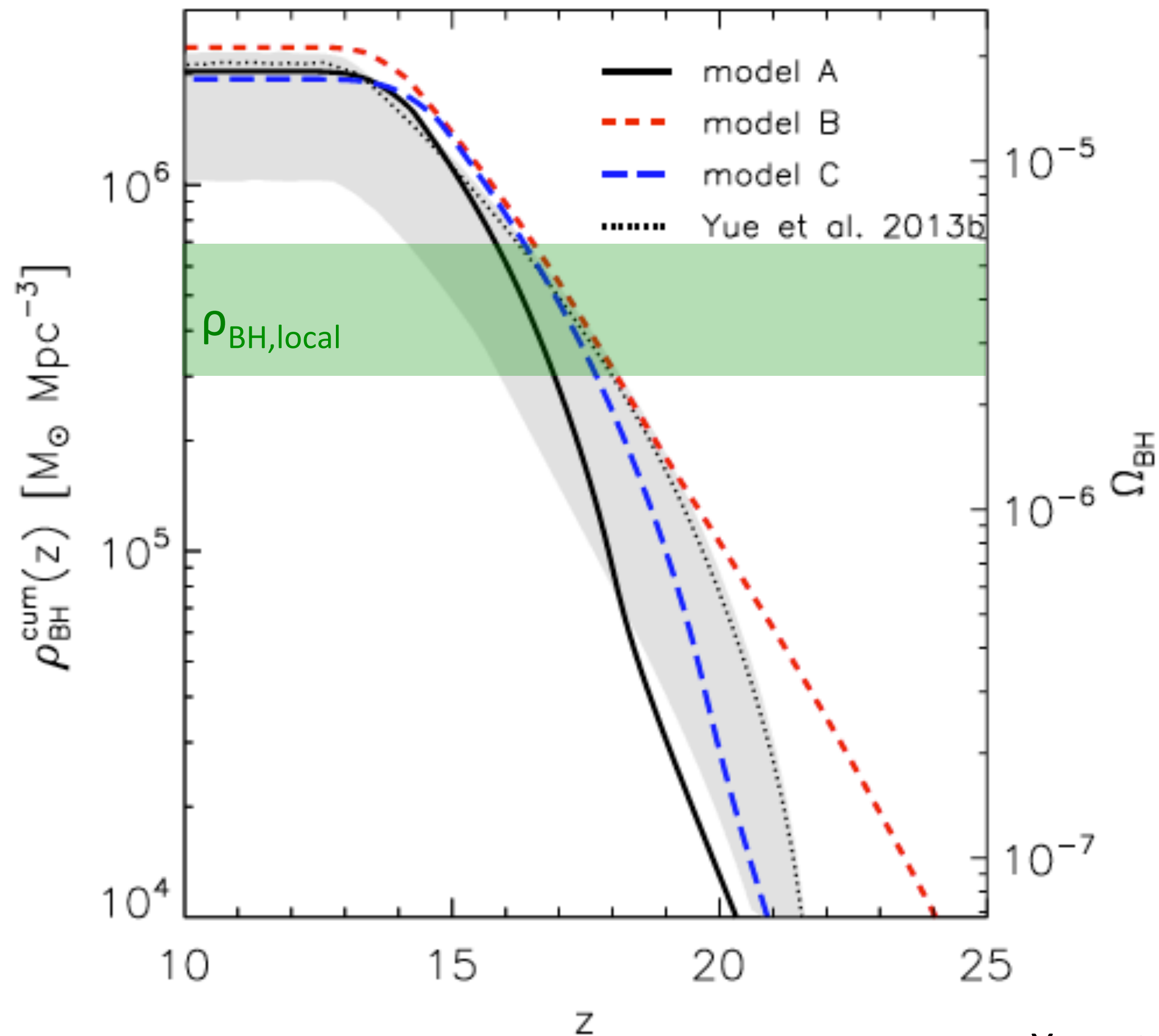

Yue et al. 2014

Are we just seeing the tip of the iceberg?
most likely yes

How many low-lum (small BHs) and distant AGN do we miss?
No BH with $M<10^7\ M_{sun}$ discovered when $t_U < 1$ Gyr

How many obscured and distant AGN do we miss?
we miss all hidden SMBHs at $z>6$, i.e. the largest population

How do we detect them and distinguish among the various seeding and fueling models?
deep multi-λ fields, cosmic bkgs, future facilities (see last lecture)